

Neuropathology

1779 SOX2 Immunorexpression in High-Grade Gliomas: Potential Marker for Targeted Therapy

G Aggarwal, S Sharma. Medical College of Georgia, Georgia Health Sciences University, Augusta, GA.

Background: Gliomas may arise from neuroectodermal stem or progenitor cells. SOX (SRY-like HMG box) genes may be of particular interest as these represent a family of transcriptional cofactors implicated in the control of embryonic development of CNS. It is highly expressed within the embryonic neuroectodermal progenitors, and is downregulated as neural cells exit the cell cycle and differentiate. SOX genes are amplified/upregulated in tumors, and Sox2 is overexpressed in malignant glioma. Sox2 silencing in glioblastoma tumor-initiating cells inhibits proliferation in mice. We aimed to study the distribution of Sox-2 positive cells in high-grade (malignant) gliomas.

Design: A total of 44 malignant gliomas (WHO grades 3 and 4) were identified from pathology archives. These were diagnosed and graded using WHO classification. These included 39 glioblastomas (GBM), 2 gliosarcomas (GS), 2 anaplastic astrocytomas (AA) and 1 anaplastic oligodendroglioma (AO). Sox2 immunohistochemistry was performed on formalin-fixed paraffin embedded tissue from these cases. The staining was reviewed for percentage positivity of tumor cells, staining intensity semiquantitatively (1+ to 4+), and various tumor patterns including positivity in infiltrating tumor cells (ITC), pseudopalisading, perivascular and pleomorphic tumor giant cells (PGC).

Results: All 44 (100%) malignant gliomas exhibited nuclear positivity of neoplastic cells. The control non-neoplastic autopsy brain tissues did not show any staining of normal cells or those in reactive gliosis. Of the tumors that showed specific patterns, 41/41 showed Sox2 positivity in ITC, 37/42 in perivascular tumor cell aggregates, 25/29 in pseudopalisading cells, and 5 had positivity in subpial accentuation. PGC were identified to be positive in 11/11 cases, including 1 GS. The sarcomatous component of GS was negative. Of note, endothelial cells in microvascular proliferation were negative. Only 11/44 (25%) showed <100% tumor cell staining varying from 5% to 90%, including 2 GS and 3 grade-3 gliomas.

Conclusions: The present study confirmed the strong immunorexpression of Sox2 in high grade gliomas, including all GBMs, and was undetectable in normal cortex. Since SOX2 immunorexpression in this study was also noted in infiltrating as well as perivascular and pseudopalisading (hypoxic) tumor cells, which are relatively refractory to chemoradiation, anti-Sox-2 targeted immunotherapy carries the potential to complement conventional therapy in high-grade gliomas.

1780 Molecular Genetic and Clinical Characteristics of Glioblastoma with Oligodendroglial Component (GBM-O)

CL Appin, CS Chisolm, C Vincentelli, C Hao, SB Hunter, DJ Brat. Emory University School of Medicine, Atlanta, GA.

Background: Glioblastoma with oligodendroglial component, WHO grade IV (GBM-O) is a recently recognized subtype of GBM (WHO, 2007) with little known of its distinguishing clinical or molecular features. Common genetic alterations in classic GBM include *EGFR* amplification (amp, 40-50%), *PTEN* deletion (del, 80-90%), and *MGMT* promoter methylation (40-50%). Chromosome 1p and 19q co-deletion (co-del) is frequent in oligodendroglomas (60-80%), but occurs in less than 5% of GBMs. Mutant *IDH1* is present in 5-10% of primary GBMs and 70-80% of secondary GBMs. Here we describe molecular genetic and clinical features of GBM-O.

Design: Results of molecular testing on GBMs diagnosed from 2008 to 2011 at Emory University were analyzed. DNA methylation of the *MGMT* promoter was determined by methylation-specific PCR. *EGFR*, *PTEN*, 1p and 19q status were determined by fluorescence in situ hybridization (FISH). Immunohistochemistry was used to determine mutant *IDH1* expression (IDH1R132H). Age at diagnosis and gender were also noted.

Results: Between 2008 and 2011, a total of 252 GBMs were diagnosed and 31 (12%) were classified as GBM-O. Patients with GBM-O were younger than those with classic GBMs (mean, 50.6 yrs vs. 58.6 yrs, respectively; Student's *t* test $p = 0.04$) and the majority were men (80% of GBM-O vs. 57% of classic GBM). *MGMT* promoter methylation status was not substantially different between GBM-O and GBM (45% vs 50%, respectively). *EGFR* was amplified in 38% of classic GBMs compared to 26% of GBM-O. Almost all (95%) classic GBMs showed *PTEN* del compared to 75% of GBM-O. Co-del of 1p/19q was noted in 31% of GBM-O. Mutant *IDH1* protein was detected in 31% of GBM-Os and 9% of classic GBMs.

Conclusions: GBM-O affects younger patients and a higher percentage of males than classic GBM. The spectrum of genetic alterations in GBM-O is slightly different than classic GBMs, with lower frequencies of *EGFR* amp and *PTEN* del and higher frequencies of 1p/19q co-del and *IDH1* mutation.

1781 The TGF-Beta Pathway: A Potential Mediator of Medulloblastoma Progression

D Aref, C Moffatt, A Perry, S Agnihotri, SE Croul. University of Toronto, Toronto, ON, Canada; University of California San Francisco, San Francisco, CA.

Background: Medulloblastoma, an embryonal neuroepithelial tumour arising in the cerebellum, is the most common malignant brain tumor of childhood. Although current treatment regimens have significantly improved survival over the past decades, recurrent and/or metastatic medulloblastoma still spells poor prognosis for patients. Aggressiveness is marked by increased growth and decreased responsiveness to available therapies. However the molecular changes that underlie these pathophysiological behaviors during medulloblastoma progression are not well understood.

Design: To further identify pathways of signaling that contribute to medulloblastoma metastasis and recurrence we decided to undertake an unbiased, whole genome expression study. We performed microarray experiments, using human patient matched

primary and recurrent or metastatic samples. This was supplemented with microarray data derived from murine samples from two different mouse models of medulloblastoma, the Ptc⁺/ and Smo⁺ models, that present with differing clinical histories and disease aggressiveness.

Results: At both the human and murine levels we identified the Transforming Growth Factor-Beta (TGF-Beta) as a potential contributor to medulloblastoma progression/metastasis. Smad3, a major downstream component of the TGF-Beta pathway, was also evaluated using immunohistochemistry in both developing and malignant human and murine tissue and was shown to correlate with disease progression. Currently we are in the process of assessing the contribution of this signaling pathway in an *in vitro* setting.

Conclusions: This work identifies TGF-Beta as a potential contributor to medulloblastoma progression and metastasis both at the level of RNA and protein expression in the human and murine species. To our knowledge, this is the first study that implicates TGF-Beta as a contributor to medulloblastoma progression and metastasis.

1782 Pathologic Features of Pleomorphic Xanthoastrocytoma, Conventional and Anaplastic: A Single Tertiary-Care Oncology Centre Experience

MM Bal, S Epari, S Kane, S Pungaonkar, A Moiyadi, P Shetty, T Gupta, N Lanke, R Jalali. Tata Memorial Hospital, Mumbai, Maharashtra, India; Nanavati Hospital, Mumbai, Maharashtra, India.

Background: Pleomorphic xanthoastrocytoma (PXA) is an uncommon low-grade glial neoplasm associated with favorable outcome. However, a subset of cases display aggressive histology and are referred to as PXA with anaplastic features (APXA). The aim of this study was to review the clinical and pathological features of conventional PXA and APXA cases.

Design: Paraffin blocks and slides of all consecutive cases of PXA accessioned during a 9 year period were retrieved. Histology was reviewed and diagnosis confirmed according to WHO 2007 classification. Clinical, radiological and follow-up details were obtained from electronic medical records and patients' files.

Results: A total of 39 cases were studied, comprising 31 PXA, grade II (79%) and 8 APXA (21%) cases. Median age was 19 years. Male-to-female ratio was 1.6:1. Temporal lobe was the commonest site involved. Rare occurrences in cerebellum and spinal cord were also observed in 2 and 1 cases, respectively. Out of 31 PXA cases, 3 cases revealed atypical morphological features of extensive microvascular proliferation (MVP) and MIB-1 labeling > 10% superimposed upon classical features of PXA. Six out of 8 APXA cases were *de novo* while 2 evolved from a pre-existing grade II PXA. Prior radiation was given in the 2 secondary APXA cases. Histologically, APXA cases were characterized by conventional PXA areas with additional presence of necrosis, MVP, augmented mitoses (mean, 8/10 HPF) and MIB-1 labeling indices (mean, 18%). Additionally, a few APXA tumors exhibited a preponderant epithelioid histology (4), rhabdoid phenotype (2) and an angiocentric pattern (1). Presence of MVP and MIB-1 > 10% was observed in the 2 primary grade II PXAs tumors that subsequently evolved to secondary APXA. Immunohistochemistry revealed S-100, focal GFAP and CD34 reactivity and absent p53 expression. Follow-up ranged from 3-47 (median, 29 months). Recurrence rate in PXA, grade II and APXA was 12% and 75%, respectively.

Conclusions: PXAs are unique glial neoplasms with a distinctive clinical and pathological profile. APXAs are higher grade PXAs that display aggressive histology and proclivity towards early recurrences and worse outcome. Microvascular proliferation and MIB > 10% appear to be a harbinger of an impending transformation of grade II PXA to APXA.

1783 Transmantle Focal Cortical Dysplasia: A Clinicopathologic Study of 12 Cases Emphasizing Histopathologic Features

MJ Cascio, DD Wang, AE Deans, AJ Barkovich, T Tihan. UCSF, San Francisco.

Background: Cortical dysplasias are a heterogeneous group of disorders that often result in pharmaco-resistant epilepsies. In epileptic patients, the incidence of focal cortical dysplasia ranges from 12-40%. Focal cortical dysplasia can be classified by pathologic and radiologic characteristics. Transmantle focal cortical dysplasia (TFCD) is a subset of focal cortical dysplasia that is defined by its distinctive neuroradiologic appearance. To date, the microscopic features of this entity have not been well characterized. In this study, we describe the detailed histopathologic features of TFCD and compare the findings with those of other focal cortical dysplasias.

Design: All cases of focal cortical dysplasia diagnosed and treated at our institution were reviewed and those that fulfilled the radiological criteria for TFCD were included in the study. An age and gender-matched control group was selected among patients with focal cortical dysplasia without radiologic criteria for TFCD. ILAE Type III cases were excluded. For each case, patient age, gender, site of lesion, clinical presentation and outcome were recorded. Histopathologic features were compared between the two groups.

Results: There were 12 patients with radiological features that fulfilled the criteria for TFCD. The group included 6 males and 6 females with a median age of 16.5 years (range, 7 months to 24 years). The lesions were identified in the parietal (17%), frontal (59%), temporal lobe (8%), and occipital lobes (8%). In one patient, the lesion was holohemispheric. Complex partial seizures were the most common presenting seizure type, with two patients demonstrating generalized tonic-clonic seizures. Gross total resection was achieved in 11 cases. Histological evaluation demonstrated dysmorphic neurons in 75%, disruption of the cortical lamination in 75%, hypercellularity in 50%, reactive gliosis in 17%, heterotopic foci in 17%, neuronal cytomegaly in 25% and balloon cells in 50%. In almost all cases there were an increased number of bizarre neurons within the deep white matter included in the resections.

Conclusions: The cardinal histological features of TFCD seem to be indistinguishable from typical focal cortical dysplasia. TFCD appeared to be more commonly associated with the presence of bizarre neurons in the deep white matter, but larger studies are

needed to substantiate this impression. We conclude that TFCO is best distinguished from other types of cortical dysplasia by its distinctive neuroradiologic appearance.

1784 Prognostic Relevance of c-Myc and Bmi-1 Expression in Patients with Glioblastoma Multiforme

T Cenci, M Martini, N Montano, S Capodimonti, R Pallini, LM Larocca. Università Cattolica del Sacro Cuore, Rome, Italy.

Background: Although the c-Myc oncogene is one of the most important and frequently deregulated proteins in different human tumors playing a central role in cell growth and apoptosis, the involvement of this gene in the pathogenesis of glioblastoma multiforme is not clear and still debated.

Design: We have analyzed the expression of c-Myc, Bmi-1 and H3K9ac, using immunohistochemistry, in 48 patients with glioblastoma multiforme (GBM) and in 20 normal brain tissues. After surgical treatment, all GBMs were subjected to adjuvant radiotherapy with concomitant administration of temozolomide. Protein expressions were correlated with clinical characteristics and outcome.

Results: We found that overexpression of c-Myc were significantly associated to Bmi-1 expression ($p=0.009$). c-Myc and Bmi-1 overexpression was significantly associated to longer overall survival ($p<0.0001$ and $p=0.0009$, respectively). In addition, within unmethylated MGMT cases treated with TMZ, GBMs overexpressing c-Myc showed a better prognosis in comparison to GBMs with normal or low expression of c-Myc ($p<0.0001$). Conversely, H3K9ac expression showed no significant association to any biological and clinical features. Multivariate analysis considering c-Myc, Bmi-1, MGMT methylation status, age, sex, Ki-67 and KPS, as variables, showed that c-Myc ($p=0.022$), Ki-67 ($p=0.036$), MGMT ($p=0.05$) and KPS ($p=0.017$) were significant predictors for favorable outcome.

Conclusions: Our results seem to reinforce the recently formulated hypothesis that c-Myc and associated genes, such as Bmi-1, could have a role in the sensitization of cancer cells towards several chemotherapeutic agents, such as TMZ, probably through the activation of different apoptotic pathways.

1785 Loss of SMARCB1/INI1 Expression in Pediatric Poorly Differentiated Chordomas

L Clark, M Gokden, AG Saad. University of Arkansas for Medical Sciences, Little Rock.

Background: Chordomas are malignant neoplasms that typically arise in adults in the axial spine. However, pediatric chordomas usually display an aggressive clinical course and show unusual histological features. We noted the absence of SMARCB1/INI1 expression by immunohistochemistry in an index case of poorly differentiated chordoma of the base of the skull in a child leading us to further study SMARCB1/INI1 immunoreactivity in 4 additional cases of pediatric chordomas.

Design: The files of the Department of Pathology at Arkansas Children's Hospital and University of Arkansas for Medical Sciences were searched for poorly differentiated chordomas occurring in children. Immunohistochemistry for SMARCB1/INI1 (Cell Marque; prediluted) was performed according to the manufacturer guidelines. Fluorescence in situ hybridization (FISH) was performed on paraffin-embedded tissue using the BAC clone RP11-8007 (Bluegnome, Cambridge, UK) the target of which are 3.4 kb distal to the SMARCB1 locus at 22q11.23. Demographic and clinical data were collected from the patients' medical records.

Results: The search resulted in 5 poorly differentiated chordomas (3 males and 2 females; median age: 12.5 years; range: 9-17 years). All cases were chordomas of the base of the skull. All cases were reviewed for the accuracy of diagnosis. By immunohistochemistry, there was loss of SMARCB1/INI1 expression in all 5 cases. In all cases, INI-1 immunoreactivity was retained in the endothelial cells serving as internal positive control and confirming the immunoreactivity of the tissue (in two cases, the blocks were in storage for more than 15 years). FISH studies were performed on 2 cases and showed evidence of deletion in SMARCB1/INI1 locus on chromosome 22q. In two cases (ages 10 and 11.7 years, respectively) the tumor cells showed moderate atypia and pleomorphism as well as large eosinophilic cytoplasm and eccentric nucleus reminiscent of atypical teratoid rhabdoid tumor. In these specific two cases, the diagnosis of chordoma was confirmed by the positivity of the tumors to brachyury, a specific marker of notochordal differentiation.

Conclusions: We report 5 cases of pediatric poorly differentiated chordoma showing loss of SMARCB1/INI1 by immunohistochemistry. Awareness of this immunoprofile of poorly differentiated chordomas is important to avoid diagnostic pitfalls. This is particularly true in those cases where the cytology resembles atypical teratoid rhabdoid tumor.

1786 Neuropathology of Patients with Multiple Surgeries for Medically Intractable Epilepsy

YB Cruz, RA Prayson. Cleveland Clinic Lerner College of Medicine of Case Western Reserve University, Cleveland, OH; Cleveland Clinic Foundation, Cleveland, OH.

Background: Surgery is a well-established treatment for patients (pts) who fail medical management of epilepsy. The success rate following surgery is generally good; however, seizures persist/recure following the initial surgery in a subset of pts. We hypothesize that in pts who require multiple surgeries for intractable epilepsy, an identifiable pathologic substrate can be found in the subsequent surgical specimen which accounts for the recurrent seizures.

Design: A retrospective study of 102 pts (56 females) with medically intractable epilepsy who have had at least 2 surgeries more than 60 days apart from 1990-2010 out of 3,157 pts who had surgery during this time interval; 15 pts had 3 or more surgeries. Pt age at time of 1st surgery ranged from 3 mos-60 yrs (mean 18.1 yrs). Duration of seizures prior to 1st surgery ranged from < 2 wks-60 yrs (mean 9.7 yrs). Time between the 1st and 2nd surgeries ranged from 0.28-15.3 yrs (mean 4.3 yrs).

Results: Pathologies at initial resection included focal cortical dysplasia (45%), tumor (19%), hippocampal sclerosis (16%), non-specific changes (13%), Rasmussen's encephalitis (6%), infarct (10%), Sturge Weber (2%), and granulomatous meningoencephalitis (1%); 10% of pts had multiple significant pathologies. Significant pathologies were identified in 84% of cases in the 2nd surgery. Of the 89 pts that had a significant initial surgical finding, 74/89 had a significant pathology at 2nd surgery; the same pathology was identified in 49/74 of these cases. The most commonly identified pathologies at 2nd surgery included remote infarcts (likely postoperative) (N=51) and focal cortical dysplasia (N=29). Three out of the 13 pts with initially non-specific findings had a significant finding at 2nd surgery, excluding post-operative infarct. Of the 15 pts who underwent a 3rd surgery, 8 had remote infarcts and 6 had recurrent/residual tumors at 3rd surgery. Follow-up after last surgery ranged from 0.5-190 mos (mean 48 mos); 83% of pts were on anti-convulsive medication and 57% were seizure-free at last known follow-up.

Conclusions: In the majority of cases of recurrent epilepsy with at least 2 surgeries (84%), specific pathological findings accounting for seizures was found at the 2nd surgery. In most cases with significant initial pathology, a similar pathology was present at the 2nd surgery (49/89, 55%). Post-operative contusional damage may account for persistent seizures following initial surgery in a subset of pts.

1787 The Troubling Differential Diagnosis of Extracerebellar Pilocytic Astrocytoma with Atypical Features and High-Grade Pediatric Glioma: Clinical, Histopathologic and Molecular Analyses of 16 Cases

M Cykowski, R Allen, K-M Fung, E Stolzenberg, T Dunn. University of Oklahoma Health Sciences Center, Oklahoma City, OK.

Background: Pilocytic astrocytoma (PA) is the most common glioma of childhood, recognized in classic form by a constellation of radiologic and pathologic findings. Rarely, PAs acquire a spectrum of atypical features (e.g., marked atypia, necrosis, infiltrative growth, elevated mitotic rate) that raises the differential diagnoses of atypical/anaplastic PA versus pediatric glioblastoma multiforme (pGBM). This study examines the histologic, immunohistochemical, and molecular features that might aid in this distinction, particularly considering the recently reported high rate of *BRAF* missense mutations in extracerebellar PAs.

Design: 10 PAs (9 atypical, 1 anaplastic, 8 extracerebellar, 4 recurrent) and 6 pGBMs were retrieved from institutional archives (1999-2011). Quantitative morphologic parameters (observer-independent Ki-67 and p53 labeling indices (LI), mitotic rate/20 hpfs) were compared using the Kolmogorov-Smirnov test. Qualitative morphologic parameters (presence of marked atypia, endothelial proliferation, atypical mitoses, and extent and pattern of necrosis) were compared using the Chi-square test. Pyrosequencing of *BRAF* (codon 600), *IDH1* (codon 132), and *IDH2* (codon 172) and dideoxynucleotide sequencing of *TP53* (exons 5-9) was performed following PCR of DNA isolated from representative tissue sections.

Results: Significant differences were seen between PAs and pGBMs in mitotic rate (PA = 4.3, pGBM = 21.2), atypical mitoses, (2/10 PAs, 6/6 pGBM), pseudopalisading necrosis (5/6 pGBMs), and Ki-67 LI (PA = 18.9 %, pGBM = 34.5 %). No other morphologic features met significance criteria, including extent of necrosis and p53 nuclear LI (only 2 pGBMs and 1 anaplastic PA had p53 LIs $\geq 50\%$ with the latter case demonstrating a *TP53* c.841G>A mutation). No *IDH1* or *IDH2* mutations were detected. *BRAF* V600E mutation was seen in 1 extracerebellar PA; upon closer examination of deeper sections this tumor was found to harbor rare, non-entrapped ganglion cells.

Conclusions: PAs with atypical/anaplastic features and pGBMs differed in select microscopic parameters, including atypical mitoses and Ki67 LIs (5/6 pGBMs having LIs $\geq 26\%$). Although reported in anaplastic PA, pseudopalisading necrosis was specific to pGBM in this series. There was considerable overlap in other histologic and molecular parameters. This case series also indicates that careful histologic review and further phenotypic study of *BRAF* V600E-mutated PAs is warranted.

1788 Molecular Profiling of Brain Metastases from Colorectal Cancer

G De Maglio, ES Lutrino, S Cernic, F Tuniz, M Casagrande, G Falconeri, G Aprile, M Skrap, G Fasola, S Pizzolito. University Hospital S. Maria della Misericordia, Udine, Italy.

Background: Brain metastasis (BM) from colorectal cancer (CRC) are reported with increased frequency, likely due to improved survival for patients with advanced disease. Furthermore surgical resection of oligometastatic disease may produce survival benefits in appropriately candidates. There is limited data suggesting that KRAS/BRAF mutations prevalence may differ depending on metastatic site and KRAS mutation status is more frequent in brain than in liver lesions. However, to the best of our knowledge specific studies addressing the molecular profile of BM from CRC are not available.

Design: We identified a cohort of 46 consecutive patients with CRC who underwent resection of BM. A total of 39 routinely processed tissue specimens were retrieved, histologically reviewed, macrodissected, and tested by pyrosequencing with Anti-EGFR MoAb response® KRAS status, BRAF, PIK3CA, NRAS (Diatech pharmacogenetics, Italy) kits according to manufacturer's instructions. KRAS has been tested for codons 12, 13, 61 and 146, BRAF for exon 15, PIK3CA for exons 9 and 20 and NRAS for codons 12, 13 and 61.

Results: Median age at time of BM biopsy was 65 yrs (35-82). Median survival following craniotomy was 163 days (4-1976). In BM from CRC, any KRAS mutation was detected in 22 patients (56.4%). Specifically, 15 patients (38.5%) harbored mutations on codon 12 (G12V, G12D, G12A, G12C, G12S), 5 (12.8%) on codon 13 (G13D and G13C), and 2 (5.1%) on codon 146 (A146V). Among patients with wild-type status for KRAS, 3 (7.7%) harbored V600E BRAF mutation. PIK3CA was mutated in 5 (12.8%) patients (4 on exon 19: E542K, E545K and Q546K, 1 on exon 20, H1047R); PIK3CA/KRAS mutations were concomitant in 3 cases. No NRAS mutations were detected. All wild-type patients were 12 (30.8%). Median survival was similar between patients

with all wild-type tumors and patients harboring any mutation in the EGFR-pathway. **Conclusions:** KRAS, BRAF and PIK3CA were identified as the main mutation targets in brain metastases. This is in keeping with known oncogene profiling studies in primary colorectal cancers. Somatic changes in the EGFR-KRAS pathway members were mutually exclusive except for PIK3CA and KRAS with no prevalence of any particular mutation. KRAS mutation rate (56.4%) in BM was higher than expected in primary CRC, as previously reported in literature.

1789 Low Rate of *IDH1* R132H Mutation in Adult Non-Supratentorial Low and Intermediate Grade Diffuse Gliomas

B Ellezam, L Heathcock, GN Fuller, JM Bruner, KD Aldape. University of Texas MD Anderson Cancer Center, Houston, TX.

Background: Diffuse gliomas (DG) are most frequent in supratentorial locations; however, they also rarely occur in the brainstem, cerebellum and spinal cord. Minute biopsies from these sites are often challenging to interpret and could benefit from diagnostic ancillary studies. Isocitrate dehydrogenase 1 (*IDH1*) mutation status has been shown to help distinguish adult low grade DG from reactive gliosis or from different CNS tumors with overlapping histologic features; however, published data on *IDH1* mutation status in DG have focused on supratentorial tumors which may not share the same biology as their non-supratentorial counterparts. The cumulative reported rate of *IDH1* R132H mutation in grade II or III DG is up to 75%.

Design: We searched our archives for cases of adult grade II or III DG involving brainstem, cerebellum or spinal cord. Cases with available archived tissue were processed for mutant *IDH1* R132H immunohistochemistry.

Results: Thirty-three cases had tissue available, including 14 from brainstem (6 diffuse astrocytomas (DA) and 8 anaplastic astrocytomas (AA)), 10 from cerebellum (2 DA, 1 low grade glioma and 7 AA) and 9 from spinal cord (4 DA, 3 AA and 2 oligodendrogliomas). The median age at diagnosis was 47 years (range 17-78). Remarkably, only 3 (9%) of 33 tumors were positive for mutant *IDH1* R132H immunohistochemistry, including 2 (20%) of 10 in the cerebellum (2 AA) and 1 (7%) of 14 in the brainstem (1 DA). None of 9 spinal cord tumors were positive for the mutant protein.

Conclusions: In contrast to the high reported rate of *IDH1* R132H mutation in supratentorial grade II or III DG, the rate in non-supratentorial cases appears very low, suggesting location-specific biology in these tumors. Genome-wide studies and mutation profiling are warranted to further explore that possibility and to exclude other *IDH1/2* mutations. The low prevalence of *IDH1* R132H mutation in non-supratentorial DG may limit its use as a diagnostic tool in this setting.

1790 Expression of Mini-Chromosome Maintenance MCM6 Protein in Meningiomas Is Strongly Correlated with Histological Grade and Clinical Outcome

G Gauchotte, C Vigouroux, F Rech, S-F Battaglia-Hsu, M Soudant, C Pinelli, T Civit, L Taillandier, J-M Vignaud, A Bressenot. CHU, Nancy, France; Medical Faculty of Nancy, Nancy, France.

Background: The 2007 World Health Organization histologic grading of meningiomas is associated with recurrence and clinical outcome. However, distinction of grade I from grade II (atypical) meningiomas can be challenging. In the WHO classification, there are 4 ways to achieve grade II status: mitotic rate, cyto-architectural features, brain invasion and/or histological subtype. Furthermore, this classification fails to detect grade I recurrent meningiomas, for which other prognostic criteria would be needed.

Design: The aim of this study was to evaluate the respective value of several markers involved in cell cycle as effective tools to predict recurrence. This retrospective study was based on a series of 59 meningiomas (grade I: 32/59; grade II: 27/59, all harboring ≥ 4 mitoses/1.6 mm²), analyzed with the following immunohistochemical markers: MCM6, Ki-67, PHH3, cyclin D1 and p53.

Results: We found a significant correlation between histologic grade and mean labeling index for MCM6 (grade I: 21.8% vs grade II: 66.4%; $p < 0.001$), Ki-67 (3.2% vs 16.3%; $p < 0.001$), PHH3 (0.7% vs 2.7%; $p = 0.010$), cyclin D1 (50.4% vs 70.0%; $p = 0.004$) and p53 (17.3% vs 32.4%; $p < 0.001$). Histologic grading and mitotic index were correlated with progression-free survival ($p = 0.010$ and $p = 0.020$, respectively). A nearly linear correlation was found between progression-free survival and staining for MCM6 ($p < 0.001$), Ki-67 ($p = 0.003$) and PHH3 ($p = 0.037$), but not cyclin D1 ($p = 0.400$) and p53 ($p = 0.763$). The inter-observer agreement coefficients for MCM6, Ki-67, PHH3, cyclin D1 and p53 were respectively 0.97 (95%CI: 0.95-0.98), 0.93 (0.89-0.96), 0.81 (0.71-0.88), 0.87 (0.80-0.92) and 0.84 (0.73-0.90).

Conclusions: In conclusion, due to its strong level of expression and sharp difference in labeling index between indolent and recurrent tumors, MCM6 is the most efficient marker to identify tumors with high risk of recurrence.

1791 The Diagnostic Utility of Brain Biopsy in Patients with Clinical Suspicion of Encephalitis and Non-Enhancing CNS Lesions

GL Genrich, J Gelfand, A Green, B Cree, T Tihan. University of California at San Francisco, San Francisco.

Background: The clinical manifestations of encephalitis are highly diverse and the differential diagnosis includes numerous infectious and noninfectious processes. Brain biopsy is an invasive diagnostic modality of last resort, in patients for whom CSF analyses and neuroimaging do not yield conclusive diagnoses. The diagnostic utility of biopsies in such cases is not well established. In patients who do undergo biopsy, the diagnosis may be interpreted as encephalitis without specific features. The clinical outcomes in this particular patient cohort are useful in determining the value of an invasive procedure in definitive diagnosis.

Design: We reviewed Department of Pathology archives for all cases submitted with a clinical suspicion of encephalitis from 1989-2010. The search algorithm identified all cases in which "encephalitis" appeared in the clinical differential diagnosis and in the final pathology report. For cases, the clinical symptoms at presentation, histopathologic features and diagnoses on brain biopsy, and follow-up information were gathered from electronic medical records and physician files.

Results: We identified 130 patients (87 males, 43 females; mean age 41 years) with a clinical suspicion and pathological diagnosis of encephalitis. The diagnoses were encephalitis, not otherwise specified (NOS) in 79 cases, specific viral encephalitis in 28 cases, toxoplasma encephalitis in 11 cases, paraneoplastic (limbic) encephalitis in 3 cases, fungal encephalitis in 2 cases, and Rasmussen's encephalitis in 2 cases. Other diagnoses included *Balamuthia sp.*, *Pseudallescheria boydii*, larva migrans, tuberculosis and granulomatous encephalitis NOS (1 case each). In the "encephalitis, NOS" group, there were 47 males and 32 females (mean age, 41 years). The "NOS" diagnosis was changed to a specific diagnosis after retrospective histopathologic review in 5 cases. Clinical follow-up revealed a specific diagnosis in 23 cases. The diagnoses could not be further specified in 51 cases.

Conclusions: The initial diagnostic yield of brain biopsies in patients with a suspicion of "encephalitis" and with diffuse radiological abnormalities without enhancement was 39%. Among the biopsies with "encephalitis NOS," a specific etiology was not determined in 51 cases after follow-up. The overall nonspecific diagnoses (39%) even after follow-up necessitates a more cautious approach to brain biopsy in encephalitis cases, and the use of an algorithm to maximize the diagnostic yield.

1792 EGFR Expression Pattern in Meningiomas

A Guillaudeau, K Durand, S Robert, F Caire, H Rabinovitch-Chable, F Labrousse. Dupuytren University Hospital and Faculty of Medicine, Limoges, France.

Background: In addition to EGFR variant I (v1) mRNA, which encodes the full-length receptor isoform α (EGFR or HER1), the *EGFR* gene is transcribed into 4 different alternatively spliced mRNAs variants referred to as variants 2 to 4 (EGFRv2 to -v4). These variants are shorter than EGFRv1 and encode truncated EGFR isoforms that lack the receptor's intracellular domain and, for two of them, a portion of the extracellular domain. The EGFRvIII mutant, encoding a constitutively active truncated receptor, is involved in gliomas oncogenesis. In meningiomas, EGFR expression pattern remains greatly unknown and studies mainly focused on EGFR isoform α and EGFRv1.

Design: In 69 meningiomas, histological tumor types and grade were determined according to the WHO classification. EGFRv1 to -v4 and EGFRvIII mRNAs were quantified by RT-PCR. Protein expression was investigated by immunohistochemistry using two antibodies: one directed against the extracellular domain recognized all the EGFR isoforms (Ext-Ab); a second one targeted against the intracellular domain only labeled EGFRv1 and -vIII (Int-Ab). Results were analyzed with respect to clinical data, histological typing, tumor grade, and patient outcome.

Results: There were 30 grade I, 32 grade II and 7 grade III. Meningiomas expressed EGFRv1 to -v4 mRNAs, but unlike in glioblastomas, EGFRvIII was not detected. EGFRv1, -v3 and -v4 mRNAs expression levels were significantly correlated. Tumor cells expressed EGFR protein and staining was stronger with Ext-Ab than with Int-Ab ($p < 0.0001$). EGFRv1 to -v4 mRNAs expression levels as well as Ext-Ab or Int-Ab staining intensities were not related to tumor type and grade. Ki67 labeling index (LI) was higher in grade III vs. grade II and I meningiomas ($p < 0.005$). Progression free survival was significantly improved in female patients, when tumor resection was evaluated as Simpson 1 or 2, in grade I vs. grade II and III meningiomas, in cases with a Ki67 LI lower than 10%, in tumors having intermediate or high Ext-Ab staining and when expression of all the EGFR variants (v1 to -v4) was high.

Conclusions: Our results suggest that all the EGFR variants and isoforms are expressed in meningiomas, except mutant vIII. In addition, high expression levels seem to be related to a better prognosis. This would suggest that the oncogenic mechanisms involving the *EGFR* gene pathway are different in meningiomas and in glioblastomas.

1793 Genetic Profiling of Orbital and Optic Nerve Meningiomas by Single-Nucleotide Polymorphism-Based Array Analysis

C-Y Ho, S Mosier, C Eberhart, CD Gocke, DAS Batista, FJ Rodriguez. The Johns Hopkins Hospital, Baltimore, MD.

Background: Meningiomas account for approximately 4% of all intraorbital tumors. Based on the location, intraorbital meningiomas can be subclassified as primary lesions thought to be derived from the intraorbital lining (Ob) or, less commonly, intracanalicular segments of the optic nerve (ON). To date, the cytogenetic features of intraorbital meningiomas have not been delineated. With the development of single-nucleotide polymorphism (SNP) arrays, a high-resolution screening method for genetic alterations in these tumors is now available.

Design: Six cases of intraorbital meningiomas including 5 cases of Ob and one case of ON meningioma were retrieved from our surgical pathology archives from 2008 to 2011. All cases included in the study were grade I based on the WHO classification. DNA was extracted from formalin-fixed, paraffin-embedded tissue (FFPE) and hybridized on the 300k Illumina SNP array.

Results: SNP array analysis showed genetic alterations in 5 of 6 (83%) intraorbital meningiomas, including 4 Ob and one ON meningioma. Four of six (67%) cases had multiple (> 1) genetic alterations. Four of five (80%) Ob meningiomas exhibited either monosomy 22 or loss of 22q. The second most frequent alteration in Ob meningiomas was deletion of 6q (3 of 5 cases; 60%), which appears to be associated with a high proliferation rate, high-grade morphology and recurrence in cranial meningiomas. Other less common alterations detected in Ob meningiomas included partial loss of 1p, monosomy 4, loss of 7p and loss of 19p. Interestingly, the only case of ON meningioma demonstrated a unique genotype with deletion of 1pter-p35.3, deletion of 2pter-p16.3, deletion 2q22.1-qter and gain of 15q21.3-qter. The latter chromosomal

aberrations are uncommon in cranial meningiomas. Additional cases are being studied to address whether ON meningiomas have a genetic composition distinct from that of Ob and cranial meningiomas.

Conclusions: Intraorbital meningiomas appear to show frequent chromosomal alterations even in grade I tumors. Compared to cranial meningiomas, Ob meningiomas display more frequent loss of 6q, which is known to be associated with progression and poor prognosis. Our study also suggests that ON meningioma could potentially be a unique clinicopathologic and molecular entity.

1794 Pleomorphic Xanthoastrocytoma: A Single Institution Experience
CM Ida, KJ Minehan, SM Jenkins, NN Laack, BW Scheithauer, C Giannini. Mayo Clinic, Rochester, MN; Mayo Clinic, La Crosse, MN.

Background: Pleomorphic xanthoastrocytoma (PXA), a rare astrocytic tumor with relatively favorable prognosis, corresponds to WHO grade II. It is currently uncertain if PXA with histological features of anaplasia, so-called "PXA with anaplastic features" (PXA-AF), should be considered anaplastic (WHO grade III).

Design: We studied 49 patients operated at (39) or referred to (10) our Institution, with histologically confirmed PXA (1950-2011). Clinical and therapeutic data and follow-up were obtained from medical records. Slides available for review in 66 tumors from 46 patients (13 with ≥ 2 resections) were reassessed for features of anaplasia, including mitotic index (MI) $\geq 5/10$ HPF, necrosis (N) and endothelial proliferation (EP). Recurrence-free and overall survival were estimated with Kaplan-Meier methods and compared between PXA and PXA-AF with log rank tests.

Results: Patients included 28M and 21F, median age at diagnosis 21.5 yrs (8-57). Tumors were supratentorial in 47 cases (43% involving temporal lobe). Seizures were the presenting symptoms in 64% of patients. Extent of tumor removal was total in 24, subtotal in 20, biopsy-only in 1 and unknown in 4 cases. Features of anaplasia (PXA-AF) were present in 16 cases (13 at first resection; 3 at recurrence), and included MI $\geq 5/10$ HPF (7), N (2), MI $\geq 5/10$ HPF + N (4), MI $\geq 5/10$ HPF + EP (1) or MI $\geq 5/10$ HPF + N + EP (2). Median follow-up was 5 yrs (0.1-29.1) and 3.4 yrs (0.1-19.3) for PXA and PXA-AF, respectively. Recurrence occurred in 19 patients: 14 PXA (39%), 4 of which also progressed to PXA-AF, and 5 PXA-AF (38%). Three (of 36) patients with PXA died of disease, and all had progressed from PXA to PXA-AF (at 0.3, 3 and 3.6 yrs from progression). Three (of 13) patients with PXA-AF died of disease (at 0.9, 1.1 and 4.7 yrs from first resection). After first resection, 10 PXA patients and 6 PXA-AF patients received radiotherapy, chemotherapy or a combination. Additional treatment generally followed recurrence. Recurrence-free 5-year survival rates were 75% and 50% ($p=0.34$) and overall 5-year survival rates were 95% and 82% ($p=0.05$) for PXA and PXA-AF patients, respectively.

Conclusions: This study confirms that overall survival is significantly decreased in PXA-AF when compared to classic PXA, raising the consideration that PXA-AF may correspond to a higher grade tumor.

1795 Histopathological Findings in the Striatum and Substantia Nigra in a Rat Model of Parkinson's Disease

S Isajevs, D Isajeva, J Pupure, J Rumaks, S Svirskis, Z Dzirkale, B Jansone, V Klusa. Faculty of Medicine, University of Latvia, Riga, Latvia.

Background: Oxidative stress and neuroinflammation play a significant role in the pathogenesis of Parkinson's disease (PD), however the cause of the neuronal loss in PD is still poorly understood. The aim of present study was to evaluate the influence of 6-hydroxydopamine (6-OHDA) on the expression on inflammatory, neuroregenerative, as well as GABAergic and cholinergic pathways biomarkers by analyzing iNOS, IL-1 β , GFAP, IBA-1, nestin, tyrosine hydroxylase, glutamate decarboxylase 65/67 (GAD65/67), acetylcholinesterase (AChE), c-jun/AP-1 and GAP-43 expression in the brain striatum and substantia nigra of animal model of Parkinson's disease (PD).

Design: PD was modeled by a single 6-OHDA intrastriatal injection in rats (20 μ g). Control group received artificial cerebrospinal fluid (aCSF). Rat brains were dissected on day 28 after discontinuation of 6-OHDA injections. The expression of iNOS, IL-1 β , GFAP, IBA-1, nestin, tyrosine hydroxylase, glutamate decarboxylase 65/67 (GAD65/67), acetylcholinesterase (AChE), c-jun/AP-1 and GAP-43 was assessed immunohistochemically and by western blot in brain striatum and substantia nigra.

Results: The obtained results showed that 6-OHDA caused an increase in GAD65/67, IL-1 β , iNOS and c-jun/AP-1 expression in rat striatum and substantia nigra (vs. control artificial CSF group). In addition, 6-OHDA increased the number of GFAP positive macroglial and IBA-1 positive microglial cells both in the striatum and substantia nigra. Obtained results showed that 6-OHDA decreased the number of AChE immunoreactive nerve fibers in striatum vs. control group (6 ± 2 vs. 23 ± 4 , $p=0.03$, fibers/mm 2), however it tend to increase AChE expression in substantia nigra. Interestingly, 6-OHDA administration upregulated GAP-43 protein expression in rat striatum, but downregulated it in substantia nigra. Our study showed a tendency of increased nestin positive cells in the rat striatum in 6-OHDA lesioned striatum, however nestin expression was not observed in substantia nigra.

Conclusions: The obtained results showed multifaceted mechanisms in the pathogenesis of Parkinson's disease that involve inflammatory, neurodegenerative as glutamate/GABAergic and cholinergic pathways.

1796 Calcifying Pseudotumor of the Neuraxis: A Review of 17 Cases

ME Jentoft, BW Scheithauer, J Shibahara, JE Parisi. Mayo Clinic, Rochester, MN; Tokyo University Hospital, Tokyo, Japan.

Background: Calcifying pseudoneoplasm of the neuraxis is a rare tumefactive calcific process that appears to be reactive in nature and involves the central nervous system, meninges, or paraspinous tissues and bone. It is morphologically distinct with amorphous variable calcified material that is often surrounded in part by a layer of mesenchymal-

appearing cells. Often a chondrocalcific appearance is present and metaplastic bone may occur. Small studies and scattered case reports indicate that these lesions follow a relatively banal post surgical course with death reported rarely. The purpose of this study is to identify the location, behavior, and associations of this uncommon lesion.

Design: Files were reviewed for cases of calcifying pseudotumor of the neuraxis that underwent surgical excision at the Mayo Clinic Rochester over an 18 year period (1992 to 2010). A review of the subjects' pathology slides and the medical record was performed.

Results: A total of 17 cases 12 (female) & 5 (male) were identified, with an average age of 58.6 (28-82) years. 5 cases were intracranial, while 12 involved the spine/paraspinous tissues with a majority of these lesions (9) involving the lower lumbar spine &/or lumbosacral junction, 2 cases involved the thoracic spine, 1 involved the lower cervical spine. 4 of the lesions appeared to be related to a distinct cause, with 2 cases being related to prior injury specifically to the region, 1 case in the field of previous radiation therapy, and 1 associated with a dysembryoplastic neuroepithelial tumor (previously reported). Follow up was available on 13 subjects with an average follow up of 78.6 (3.4-195.3) months. No cases recurred; however 1 case at the foramen magnum had a residual lesion due subtotal resection because of proximity to a vertebral artery. This lesion has not increased in size or had worsening of symptoms with 22.1 months of follow up. 3 (of 13) died, but all were due to unrelated causes.

Conclusions: Calcifying pseudoneoplasms of the neuraxis is a rare lesion, cured by gross total removal, and may be associated with previous injury or an underlying neoplasm. Though these lesions appear to follow a relatively benign course, impingement or involvement of critical structures may prevent complete surgical removal.

1797 Pilocytic Astrocytomas with Infiltrating Patterns of Growth Carry a High Rate of BRAF V600E Mutation

G Kandala, S Bannykh, S Fan, K Baden, A Pau, L Baden, P Fournier, E Thorpe, K Porpora, J Mirocha, K Kawachi, A Riley-Portuges, J Lopategui. Cedars-Sinai Medical Center, Los Angeles, CA.

Background: Pilocytic Astrocytoma (PA), a WHO grade I tumor, shows two frequent alterations in BRAF oncogene. The V600E point mutation, which is the most common tumor-associated alteration in the BRAF gene and an alternative BRAF activating mechanism that involves BRAF-KIAA1549 gene fusion with corresponding duplication at chromosome band 7q34. Although the majority of PAs are well circumscribed, a subset shows an invasive pattern akin to biologically different infiltrative gliomas. We investigated whether the presence of a BRAF point mutation and/or duplication in PAs correlate with an infiltrating pattern of growth.

Design: We identified 19 cases of PAs with brain infiltration (5 from NF1 patients) and matched them with 18 localized PAs for a total of 37 cases. Infiltration was assessed by histology and MRI. 26 cases were in adults and 11 in children.

V600E mutation was identified by an allelic discrimination PCR mutational kit. Corriel Repository HBT-38 cell line was used as a positive control. FISH studies utilized Abbott Molecular kit with probes for both CEP7 (Green) and 7q34 BRAF containing region (Gold). In each case, 50 cells were evaluated. In the cells with two green signals, presence of two gold signals indicated wild type whereas three a duplication. Cases with over 20% of cells with a gain of BRAF were scored positive for duplication. Both tests were done on all cases.

Statistical analysis was performed using two group Fisher's-exact test of equal proportions. This compared infiltrative vs non-infiltrative tumors with V600E mutation.

Results: BRAF abnormality by either PCR or FISH was seen in 17/37 cases. The V600E mutation and the gene duplication were mutually exclusive except for one case. 6 cases showed a V600E mutation. Strikingly, 5/6 cases with the point mutation showed distinct brain infiltration. 5/14 infiltrating PAs (excluding patients with NF1) had the V600E mutation, whereas only 1/18 non-infiltrating tumors had this pathogenic point mutation. This difference attained a p-value of 0.064 by using Fisher's-exact test of equal proportions. Duplication of the BRAF gene was seen in 12/37 cases. In contrast to V600E mutation, the duplication was non-discriminatory in respect to infiltration of the PAs. Of 5 tumors in NF1 patients, one was positive for duplication and none for point mutation.

Conclusions: 1. Presence of BRAF V600E mutation appears to correlate with an infiltrating pattern of PAs in non-NF1 patients.

2. Duplication of the BRAF gene in PA is present in both infiltrative and localized tumors.

3. BRAF abnormalities are rare in NF1 PAs.

1798 Synovial Sarcoma of the Nervous System: A Clinicopathologic Study of 9 Patients

J Keith, S Croul, L Ang. Sunnybrook Health Sciences Centre, Toronto, Canada; University Health Network, University of Toronto, Toronto, Canada; London Health Sciences Centre, University of Western Ontario, London, Canada.

Background: Synovial sarcoma of the nervous system is rare, with only small case series described, and their clinicopathologic features are thus poorly understood.

Design: We reviewed the clinicopathologic features of 9 patients with synovial sarcoma affecting the nervous system. The clinical information and molecular studies were reviewed retrospectively, and a central pathology review was performed including immunohistochemistry for CK (LMW, pan, 7 and 19), EMA, S100, CD34, bcl2, CD99, and Ki67.

Results: The patients were 6 males and 3 males with a median age of 52 years (range 46-74 years). The most common tumour site was spinal nerve (C3-C5, T6, T10 and T12 in 4 cases), followed by the brachial plexus (2 cases), with single cases of the femoral nerve, tibial nerve and sacrum. 8 were primary synovial sarcomas of the nervous system with 1 metastasis from a thoracic primary. 2 cases occurred in patients with previous neurofibroma or Neurofibromatosis Type 1. Most of the lesions were large and enhancing on neuroimaging, were incompletely surgically resected, and recurred after several years (range 1-7 years, average interval to recurrence of 3.4 years). Central pathology

review of 12 tumours from 9 patients showed 9 tumours to have a monophasic fascicular growth pattern of oval pleomorphic cells with hemangiopericytomatous vasculature, and myxoid change was present in 4 tumours, prominent in 1. The 3 biphasic synovial sarcomas had a predominantly glandular morphology. The mean mitotic rate was 18 mitoses/10hpf (range of 2-50 mitoses/10 hpf). All tumours had expression of at least 1 of CK (LMW), panCK, or EMA, with panCK being the most commonly expressed antigen (78%). Molecular testing confirmed an SYT/SSX translocation in all cases in which it was performed.

Conclusions: Synovial sarcomas affecting the nervous system are rare, but are usually primary tumours of spinal or peripheral nerves with an aggressive clinical course. Their histology includes monophasic tumours with frequent myxoid change and biphasic predominantly glandular tumours, and they immunolabel with CK or EMA. Recommendations for distinguishing this entity from the major differential diagnosis, MPNST, are made, and the importance of molecular testing is emphasized.

1799 Promoter Methylation of Wnt Inhibitory Factors and Expression Pattern of Wnt/beta-Catenin Pathway in Human Astrocytoma: Pathologic and Prognostic Correlations

S-A Kim, SK Khang. University of Ulsan College of Medicine, Asan Medical Center, Seoul, Korea.

Background: Wnt inhibitory factor-1 (Wif-1) is an antagonist that inhibits Wnt signaling pathway. Thus, the functional loss of Wif-1 can contribute to tumorigenesis by activation of Wnt pathway. In this study, we investigated the contribution of Wif-1 hypermethylation to the regulation of Wnt/beta-catenin signaling pathway, tumor grade and patient survival in astrocytoma.

Design: We selected 88 astrocytoma samples consisting of 20 diffuse astrocytomas (DA) and 66 glioblastomas (GB). For control sample, 17 temporal lobectomy specimens from patient with epilepsy were selected. DNA was extracted from paraffin-embedded tissue and ratio of methylated DNA to total methylated and unmethylated DNA (%methylation) was measured by methylation and unmethylation-specific PCR. Representative tumor tissue was immunostained with Wif-1, beta-catenin, cyclin D1 and c-myc.

Results: The mean %methylation of tumor (DA and GB) were significantly higher than in control brain tissue from temporal lobectomy. Significant negative correlation between %methylation and Wif-1-positive cell percentage was noted. Mean Wif-1 IHC score were lower in %methylation \geq 10 group than in %methylation<10 group. Cyclin D1 expression was higher in %methylation \geq 10 group ($p=0.037$). However, the staining pattern of beta-catenin and the intensity of c-myc staining were not related to Wif-1 promoter methylation level. Tumors with cytoplasmic or cytoplasmic-nuclear beta-catenin staining pattern was more frequently observed in tumors containing less than 50% of Wif-1 positive cells, and in tumors with lower IHC score. No significant relation between Wif-1 protein expression level and cyclin D1 and c-myc were found. On multivariate survival analysis, decreased Wif-1-positive cell percentage and Wif-1 IHC score were independently significant factors for poorer patient survival along with higher tumor grade, increased patient age and presence of residual tumor after resection.

Conclusions: Promoter methylation level of Wif-1 gene was increased in astrocytoma and may play a role in early stage of tumorigenesis by suppressing Wif-1 expression and increasing cyclin D1 expression. Decreased Wif-1 protein expression was associated with increased accumulation of cytoplasmic or cytoplasmic-nuclear beta-catenin and plays a key role in prognosis of patients with astrocytoma.

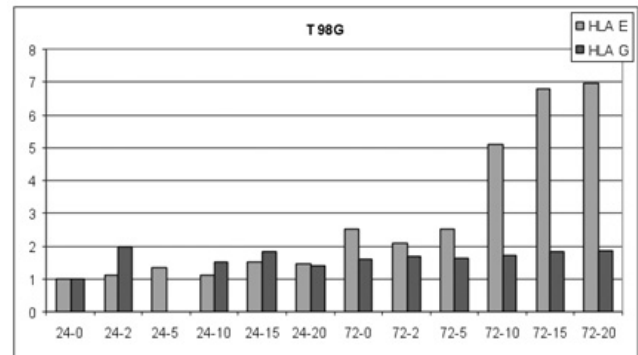
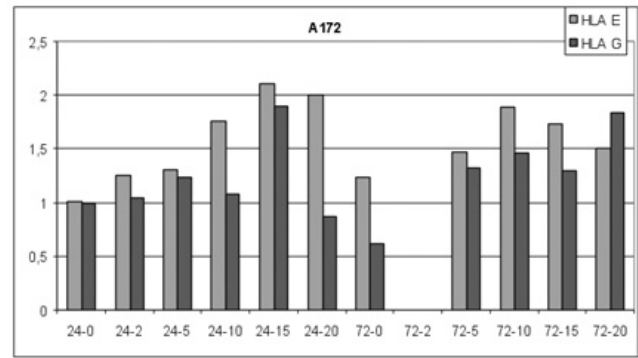
1800 Ionizing Radiation Alters the Expression of Multifunctional Immune-Modulatory Protein HLA-E in Glioblastoma Cells Lines: An Unrecognized Effect of Radiation Therapy?

L Kren, O Slaby, S Sevcikova, L Kubiczkova, M Smrcka. University Hospital Brno, Brno, Czech Republic; Masaryk Memorial Cancer Institute, Brno, Czech Republic; Medical College, University of Masaryk, Brno, Czech Republic.

Background: Immune-modulatory proteins HLA-G and HLA-E were originally thought to be restricted to the protection of the fetus from maternal allorecognition. Now they are known for multiple immune-regulatory functions. We already described production of immune-modulatory molecules HLA-G and HLA-E by both microglial cells (Kren, L. et al., *J Neuroimmunol* 2010) and neoplastic cells (Kren, L. et al. *Neuropathology* 2011). We described the unexpected positive correlation of HLA-E expression by neoplastic cells in glioblastoma (GB) with the length of survival, which we hypothesized could be attributable to subsequent therapeutic modalities. Therefore, we decided to analyse the expression of HLA-G and HLA-E in three GB cell lines before and after the impact of ionizing radiation.

Design: We used three GB cell lines: T 98G, A172 and U 87MG. The expression of HLA-G and HLA-E was assessed before application of ionizing radiation (0-2-5-10-15-20 Gy) and then was analysed again 24h and 72 h after radiation. HLA-G and HLA-E antigens were analysed flow-cytometrically.

Results: The expression of both HLA-G and HLA-E by all three cell lines of GB was elevated significantly after irradiation, especially expression of HLA-E in the line T 98G.



Conclusions: We revealed that expression of HLA-G and HLA-E in GB cell lines alters significantly after the impact of ionizing radiation. This finding may represent a new, unrecognized pathway of the effect of ionizing radiation in cancer therapy. In GB, namely, HLA-E may function, in its elevated levels, as a ligand for activating receptor CD94/NKG2C, therefore mediating increased lysis of tumor cells.

1801 Immunohistochemistry of Pediatric CNS Tumors: Mutated IDH1 and the Hippo Pathway

M Martinez-Lage, LM Sullivan, M Santi. Hospital of the University of Pennsylvania, Philadelphia, PA; The Children's Hospital of Philadelphia, Philadelphia, PA.

Background: Mutations of IDH1 are implicated in adult gliomas, rarely in children. Conversely, the hippo signaling pathway may be involved in brain tumors common in children. We report the frequency of R132H IDH1 mutations and evaluate components of the hippo pathway (CD44, NF2/merlin and YAP-1) in a series of pediatric CNS tumors.

Design: We analyzed 143 pediatric CNS tumors using tissue microarrays: 26 medulloblastomas/PNET, 21 pilocytic astrocytomas, 14 astrocytomas, 13 gangliogliomas, 12 glioblastomas, 12 ependymomas, 11 choroid plexus tumors, 10 meningiomas, 8 DNET, 8 oligodendrogliomas, 4 craniopharyngiomas, 2 germinomas, and 2 central neurocytomas. We interpreted positive staining as follows: cytoplasmic for mutated IDH1, membranous and/or cytoplasmic for CD44 and NF2/merlin (weak vs strong), and nuclear for YAP-1 (1-10% low vs >10% high).

Results: Mutated IDH1 expression was seen in 1/28 diffuse gliomas (3.6%), an oligodendroglioma with 1p19q co-deletion, and in 1/13 gangliogliomas (7.7%). CD44 was widely expressed in glial and glioneuronal neoplasms, germinomas, craniopharyngiomas and meningiomas (75-100%), whereas expression was less frequent in medulloblastoma/PNET (55.5%) and neurocytomas (50%). Strong expression was seen in gangliogliomas and pilocytic astrocytomas. NF2/merlin was frequently seen in gliomas, DNET (strong), ependymomas, neurocytomas, choroid plexus tumors, meningiomas, medulloblastoma/PNET and gangliogliomas (77-100%), but was less often seen in germinomas (37%). YAP-1 showed frequent high expression in choroid plexus tumors, ependymomas and meningiomas, and frequent low expression in DNET, pilocytic astrocytomas, diffuse astrocytomas and glioblastomas (75-100%). Oligodendrogliomas, neurocytomas, craniopharyngiomas, gangliogliomas and germinomas expressed YAP-1 in 50-67%, while 37% of medulloblastomas expressed YAP1 with a tendency to show high expression and no association by subtype.

Conclusions: 1) R132H IDH1 mutations are rare in childhood gliomas, and positive cases may behave as adult neoplasms, while the majority follows IDH-independent pathways. 2) YAP-1 and hippo related proteins CD44 and NF2/merlin play a role in a wide range of pediatric brain tumors. 3) High YAP1 expression in ependymomas and meningiomas, with weak NF2/merlin expression is relevant given the predisposition of patients with NF2 to develop these tumors, and possibly reflects downstream upregulation of YAP1 secondary to NF2/merlin deficiencies.

1802 Promoter Methylation-Associated Loss of ID4 Expression Have a Prognostic Relevance in Glioblastoma Multiforme

M Martini, T Cenci, N Montano, V Cesarini, R Pallini, LM Larocca. Università Cattolica del Sacro Cuore, Rome, Italy.

Background: Inhibitors of DNA binding/differentiation (ID1-4) are a family of helix-loop-helix transcription factor, highly expressed during embryogenesis and at

lower levels in mature tissues. Expression of ID proteins have related to features of malignancies, including cellular transformation, metastasis and angiogenesis. ID4 plays an important role in neuronal stem cell differentiation and its deregulation has been implicated in glial neoplasia. Recent works have shown that hypermethylation of ID4 can determine the silencing of this protein in several human cancers.

Design: We analyzed the methylation status of ID4 by methylation-specific-PCR in 65 glioblastoma multiforme (GBM) cases and in 20 normal brain tissues. After surgical treatment, all GBMs were subjected to adjuvant radiotherapy with concomitant administration of temozolomide. Methylation status of ID4 was confirmed by sequencing after subcloning and RNA and protein expression was assessed by real-time PCR and immunohistochemistry. We also evaluated the mRNA expression of MGP (Matrix GLA protein). The relationship between ID4 methylation and clinical outcome was investigated.

Results: The promoter of ID4 was methylated in 17/65 (26%) GBMs. After subcloning, the methylation was confirmed by sequencing in over 95% of GpC dinucleotides. In methylated GBMs, ID4 mRNA expression was reduced 5 folds as compared with unmethylated GBMs. A significant reduction of protein expression was detected in all hypermethylated cases. Moreover, GBM with ID4 methylation showed a reduced MGP mRNA expression by 2 folds in comparison to GBM with unmethylated ID4. ID4 methylation was significantly associated with a favourable clinical outcome ($p=0.0075$). No significant differences were found between patients with and without ID4 methylation with respect to age, sex, p53 mutation, Ki67 labeling index and extent of surgical resection.

Conclusions: Our data suggest that methylation of ID4 may be involved in the pathogenesis of GBM probably playing a role on MGP mediated neoangiogenesis, and in the resistance of this neoplasm to conventional treatment.

1803 Diagnostic Application of Genetically Distinct Medulloblastomas

HS Min, S-K Kim, JY Lee, SH Park. Seoul National University College of Medicine, Seoul, Korea.

Background: Recent analysis on genetic features of medulloblastoma (MB) could classify it into 3 to 4 subgroups according to the gene expression profiles, including the Wnt signaling pathway-activated group (WNT), the Sonic Hedgehog signaling pathway-activated group (SHH) and the group showing neural/photoreceptor differentiation (non-WNT/SHH). These molecular features reflect the distinct developmental origin of MB and correlate with some clinicopathologic traits. To apply this to the practical diagnosis and to contribute the risk stratification, the present study analyzed 75 MBs subjected to immunohistochemistry (IHC) and fluorescent in situ hybridization (FISH), in addition to the array-based comparative genomic hybridization (array CGH).

Design: Clinicopathologic review of 75 MBs from the archive of Seoul National University Hospital (1999-2009) was carried out. IHC was done in all cases for β -catenin, YAP1, GAP, filamin A, SFRP1, Eomes. Array CGH were performed in 36 cases by GenomArray (Macrogen Inc, Korea). FISH analysis was performed using commercially available digoxigenin-labeled cosmid probes for MYC (8q24.12-q24.13), MYCN (2p24), CEP2 (2p11.1-q11.1), CEP8 (8p11.1-q11.1), LIS1 (17p13.3), and RARA (17q21) from Vysis and MYB (6q23, Abott).

Results: The median age of patients was 13 years old (range: 1-30 yrs) and M:F ratio was 2.9:1 with 32% (24/75) mortality. Both filamin A and YAP1 were expressed in 6 cases, suggested as WNT group (8%). It included 5 classic and 1 desmoplastic/nodular (D/N) MB. 13 cases (17.4%) were suggested as SHH group showing positivity of filamin A, YAP1 and GAB, which included 8 D/N and 3 classic type. Two cases of large cell/anaplastic (LC/A) MB also showed positivity for these 3 markers. The non-WNT/SHH 56 cases (75%) comprised 40 classic, 9 D/N and 6 LC/A subtype. In array-CGH, 17/36 (47.2%) cases showed chr.17 aberrations (mostly i17q), 82.4% of which revealed chr. 7 gain and/or 8 loss. Chr.17 aberrations were observed in 17 cases correspondingly by FISH, and MYC/MYC amplification were found in 1 and 3 cases, respectively. SHH subgroups showed the better survival than non-WNT/SHH subgroup ($p=0.006$), and i17q, 7 gain and/or 8 loss were significantly associated with poor clinical outcome ($p<0.02$, $p<0.001$).

Conclusions: From our study, we suggest that IHC for filamin A, YAP1 and GAB can be applied for the subgrouping of MB, but it can be supplemented by monosomy 6 using FISH and β -catenin or PTCH1 mutation study. Chr.7 gain and/or 8 loss are suggested as strong indicators of poor clinical outcome.

1804 Malignant Epidural Spinal Cord Tumor with Neuroendocrine Differentiation Associated with EWSR1/ATF1 Fusion Transcript

CA Mohila, A Olar, A Roy, MD Weindel, AH Jea, M Chintagumpala, D Lopez-Terrada, AM Adesina. Texas Children's Hospital and Baylor College of Medicine, Houston, TX; The Methodist Hospital, Houston, TX.

Background: Epidural spinal cord tumors in children are relatively rare. They can arise from bone, dura, or soft tissues and in the pediatric population include neuroblastoma and Ewing's sarcoma among others. We report a case of a previously healthy 10 year old girl who presented with a 10-day history of bilateral lower extremity numbness with episodes of falling. Imaging revealed a large extradural thoracic mass compressing the spinal cord.

Design: Tumor tissue was formalin-fixed and paraffin-embedded. Sections were stained with H&E and a panel of antibodies against multiple antigens. Fluorescence in situ hybridization (FISH) using a break-apart probe specific for EWSR1 and reverse transcription polymerase chain reaction (RT-PCR) using specific primers for EWS/FLI1, EWS/ERG, EWS/ATF1, EWS/CREB1, and EWS/WT1 fusion transcripts were performed on tumor tissue.

Results: Histologic examination revealed a tumor composed of infiltrative malignant epithelioid cells with nodular and organoid arrangements. Tumor cells were

immunoreactive for synaptophysin, vimentin, EMA, CD99, and low molecular weight cytokeratin and a subset of sustentacular-like cells were positive for S100. Ultrastructural studies revealed poorly differentiated cells with scattered membrane-bound dense core granules. Together these features showed a poorly differentiated tumor with neuroendocrine features consistent with a malignant paraganglioma. FISH demonstrated an EWSR1 gene rearrangement and RT-PCR detected the presence of a EWSR1/ATF1 fusion transcript.

Conclusions: Once thought to be a tumor-defining molecular signature for clear cell sarcoma, EWSR1/ATF1 transcript has also been described in angiomatoid fibrous histiocytoma. The present case is the first to expand the spectrum of tumors with EWSR1/ATF1 fusion to include malignant tumors with neuroendocrine differentiation.

1805 Morphologic Correlates of the Alternative Lengthening of Telomeres (ALT) Phenotype in High Grade Astrocytomas

DN Nguyen, CM Heaphy, RF de Wilde, B Orr, CG Eberhart, AK Meeker, FJ Rodriguez. Johns Hopkins Medical Institutions, Baltimore, MD.

Background: Recent studies have highlighted the occurrence of a telomerase-independent mechanism of telomere maintenance known as "alternative lengthening of telomeres" (ALT) in subsets of human cancers. An increased frequency of ALT has been described in infiltrating gliomas in particular, and associated with *ATRX* mutations. We retrospectively reviewed high grade astrocytomas to uncover correlations between ALT, *ATRX* expression, histology and molecular alterations typical of infiltrating astrocytomas.

Design: We studied 117 high grade astrocytomas with available ALT status (19 WHO grade III and 98 WHO grade IV tumors). Histologic review was performed, as well as immunohistochemistry for *ATRX*, *DAXX*, and mutant *IDH1* protein. *EGFR* amplification was evaluated by Fluorescence in situ hybridization (FISH). Molecular and immunohistochemical studies were performed using tissue microarrays, while histologic evaluation was performed in whole H&E sections in a subset of cases with available slides ($n=37$). Oligodendroglial neoplasms were excluded from analysis.

Results: ALT was identified in 40 cases (34%), including 17 (89%) grade III astrocytomas, and 23 (24%) grade IV astrocytomas. When focusing on histologic subtypes, all small cell astrocytomas ($n=6$) and the single giant cell astrocytoma were ALT negative. The ALT phenotype was also correlated with the presence of round cells, fine chromatin, and microcysts, although these features were almost always present in grade III tumors. The ALT phenotype was positively correlated with the presence of *IDH1* mutant protein ($p<0.0001$), *ATRX* protein loss ($p<0.0001$), and absence of *EGFR* amplification ($p=0.004$). There was no significant correlation with *DAXX* expression.

Conclusions: ALT represents a specific phenotype with distinctive pathologic and molecular features. Further studies are needed to clarify the clinical and biological significance of ALT in high grade astrocytomas.

1806 Expression Status of IDH1 Mutant and SDHB Genes in Adult and Pediatric Gliomas

R Nobrega, R Patrocinio, PP Aung, J-P Lai, Z Wang, M Miettinen, K Warren, M Quezado. National Cancer Institute, National Institutes of Health, Bethesda, MD; BIOPSE Laboratory, Ceara, Brazil; Faculdade de Medicina Christus, Ceara, Brazil.

Background: Isocitrate dehydrogenase 1 (*IDH1*) and Succinate dehydrogenase (*SDH*) -mutant tumors may express increased HIF stability, which leads to a tumoral pseudohypoxic profile. Increased HIF levels may promote tumor progression by the activation of numerous cellular processes including resistance against apoptosis, vascular remodeling and angiogenesis as well as metastasis. High levels of *IDH1* mutations have been frequently detected in adult but not in pediatric gliomas. *SDH* gene mutation/expression profiles have not been extensively investigated in brain gliomas. To further explore the profile and possible relationship of these metabolism genes in gliomas tumorigenesis, we have investigated the expression of *IDH1*-mutant and *SDH-B* in a group of pediatric and adult gliomas by immunohistochemistry.

Design: Samples from 53 patients with gliomas were evaluated. H&E slides were reviewed for confirmation of diagnosis. There were 13 diffuse pontine brain glioma patients (autopsy material), and 40 gliomas in adult patients: 18 low grade (8 astrocytomas, 3 oligodendrogliomas, 2 oligoastrocytomas, 5 ependymomas), 5 high grade oligodendrogliomas, and 17 glioblastomas (GBMs). Immunohistochemistry was done for *IDH1* mutant (1:250 citric buffer, pH 6.0, Dianova) and *SDHB* (1:1000, EDTA, pH 8.0, Abcam)

Results: Pediatric brain stem gliomas were negative for mutant *IDH1* (0/13) and their *SDHB* expression was intact (13/13). *IDH1* mutant tumors included 11 low grade gliomas (5 astrocytomas, 2 oligodendrogliomas, 3 ependymomas, 1 oligoastrocytoma), 3 high grade oligodendrogliomas and 10 GBMs. No adult glioma exhibits *SDHB* loss (40/40).

Conclusions: As previously reported, *IDH1* mutations are frequently present in low and high grade gliomas and secondary GBMs in adults, but not in pediatric gliomas. No gliomas, pediatric or adult, express *SDHB* loss/mutation. It appears by our study that the *IDH1* but not the *SDH* metabolism gene is likely to be involved in HIF stabilization in brain tumors. It is unlikely that *SDH* deficiency contributes to glioma tumorigenesis.

1807 Efficacy of Transplant Media for Muscle Biopsy Sample Preservation

KO Ojemakinde, JD Wilson. Louisiana State University Health Sciences Center, Shreveport, LA.

Background: One of the limitations in the pathologic evaluation of muscle biopsy is the time interval between the biopsy procedure and the snap freezing of the sample. Timely freezing of the sample in liquid nitrogen cooled isobutane not only gives excellent frozen section morphology, but also preserves tissue biochemistry and nucleic acids. The latter

allow for accurate enzyme histochemical staining and/or subsequent biochemical and genetic testing. Institutions that refer muscle samples to a specialist are often too far to transport these time-sensitive specimens by courier and/or do not have the capability to snap freeze the muscle biopsy on premises.

Transport media are used to preserve organ donor explants during shipment. A prior report indicates that use of transport medium preserved the enzyme histochemistry of pig muscle biopsy samples for up to five days. We assessed the preservation quality of two transport media on human muscle.

Design: Skeletal muscle tissue was sampled from freshly amputated leg specimens. The samples were divided into five portions in each of the two transport mediums ("Belzer UW Cold Storage Solution" and "Lifor ACF perfusion media"), and Carnoy's fixative. One portion was snap frozen in liquid nitrogen cooled isobutane immediately. The remaining four were placed in a sterile conical tube containing 50ml of transport medium or Carnoy's fixative, and refrigerated at 4 degrees centigrade. One portion of muscle per each successive day (days 2 through 5) was snap frozen from each transport medium or preservative. Frozen sections from each of the five samples were cut and stained at the same time. Staining included hematoxylin and eosin, modified Gomori Trichrome, PAS and PASd, and enzyme histochemistry. The enzyme histochemical stains included ATPase at pHs 9.4 and 4.3, NADH-TR, alkaline phosphatase, acid phosphatase, cytochrome oxidase, succinic acid dehydrogenase, and myophosphorylase.

Results: Both transport media preserved enzymatic activities and provided good frozen section morphology for up to 5 days. Compared to the standard frozen biopsy specimens, biopsies processed from transport media contained some artifacts, such as cell shrinkage and/or tissue edema. Lifor ACF perfusion media showed somewhat more tissue edema than Belzer UW Cold Storage Solution. The sample preserved in Carnoy's fixative did not perform well.

Conclusions: Our results confirm that organ transplant media represent a viable solution for preserving muscle biopsies for morphologic and enzyme histochemical assessment.

1808 Central Nervous System Involvement by Myeloid Sarcoma

A Olar, TD Stein, CJ Davidson, A Perry, G Gheorghe. The Methodist Hospital, Houston, TX; Boston VA Medical Center, Boston University School of Medicine, Jamaica Plain, MA; Massachusetts General Hospital, Harvard Medical School, Boston, MA; Children's Hospital of Wisconsin, Medical College of Wisconsin, Milwaukee, WI; University of California, San Francisco, San Francisco, CA.

Background: Myeloid sarcoma (MS) is an extramedullary hematopoietic neoplasm of myeloid origin. Central nervous system (CNS) involvement by MS is unusual. We report ten cases of biopsy-proven CNS MS.

Design: The pathology records across eight institutions were searched for CNS MS. The clinical course, radiology and pathology were reviewed.

Results: Our results are summarized below.

| # | Age y/Sex | Associated hematologic neoplasia | Cytogenetics | CNS involvement | Other sites of involvement | CSF | Survival/mo |
|----|-----------|----------------------------------|------------------------|--|--|-----|-------------|
| 1 | 0.5/M | AML | Trisomy 8 | L FP | - | + | AWD/12 |
| 2 | 3.9/F | AML | N/A | R F | - | + | N/A |
| 3 | 16/M | AML | Inv16 | R FP | - | - | ANED/8 |
| 4 | 37/F | AML | Normal | R O | N/A | N/A | D |
| 5 | 48/F | CML | t(9;22) | R S1-S2 foramina | R sacrum | N/A | D/2 |
| 6 | 53/M | N/A | N/A | Multiple cervical and thoracic spinal cord roots | Cervical and thoracic paraspinal soft tissue | N/A | A |
| 7 | 64/M | AML | 5q del | T6-T9 bilateral neural foramina and epidural space | T6-T9 paraspinal soft tissue | N/A | D/4 |
| 8 | 69/F | PV | Complex; JAK2 mutation | L F dura | - | + | D/3 |
| 9 | 76/M | MDS | Trisomy 21 | Choroid plexus, pituitary | Widespread | N/A | D/8 |
| 10 | 84/F | MDS | Normal | L FT | - | N/A | D/<6 |

AML-acute myeloid leukemia, CML-chronic myelogenous leukemia, PV-polycythemia vera, MDS-myelodysplastic syndrome, L/R-left/right, F/P/T/O-frontal/parietal/temporal/occipital lobe, A/WD/NED-alive/with disease/no evidence of disease, D-deceased

Four patients had a prior diagnosis of a myeloid neoplasm. In 5 patients (#1, 3, 4, 7, 8) CNS MS was the initial presentation. Three (#1, 3, 4) presented with hemorrhagic masses, one of which was clinically misdiagnosed as subdural hematoma. Two (#7, 8) had enhancing lesions, one (#8) presenting with a dural-based mass. In one case (#9), MS was diagnosed at autopsy. In our series, MS occurred in isolation, sparing other organs in 6/10 cases.

Conclusions: The clinical and imaging characteristics of CNS MS overlap with those of hemorrhage and primary CNS tumors. Differential diagnosis with intracranial bleeding is particularly challenging. It is important to maintain a high index of suspicion and perform a biopsy whenever clinically appropriate. A meticulous workup is necessary to avoid misdiagnosis of other hematopoietic or nonhematopoietic neoplasms. Since CNS MS is curable, timely recognition is paramount.

1809 Immunohistochemical Analysis of IMP3 Expression in Pilocytic Astrocytomas, Glioblastomas, and Recurrent Glioblastomas

DM Patel, X Fan. Cedars-Sinai Medical Center, Los Angeles, CA.

Background: Insulin-like growth factor II mRNA-binding protein 3 (IMP3) is an oncofetal protein linked to tumor aggressiveness and has been observed in a variety of malignant neoplasms. This study aims to characterize IMP3 expression in pilocytic astrocytoma (PA), glioblastoma multiforme (GBM), and recurrent GBM and to determine if IMP3 immunostain will have diagnostic value in differentiating PA from GBM in small specimens.

Design: 21 cases of PA and 38 cases of GBM were studied. Of the GBM group, 18 cases were evaluated for both initial GBM and then recurrence. IMP3 immunostaining was performed on one representative tumor block from each case. The staining intensity (1-3+), percent of positive tumor cells, and staining pattern, along with endothelial positivity, were recorded. 5% or greater staining of tumor cells was considered positive.

Results: IMP3 positivity was found in 2 of 21 cases (9.5%) of PA, 22 of 38 cases (58%) of GBM, and 9 of 18 cases (50%) of recurrent GBM, with the difference between PA and GBM being statistically significant ($p=0.0003$). Patterns of IMP3 staining in tumor included: perivascular accentuation, subarachnoid and subpial accentuation, and scattered single cells. 2 cases of normal brain used as controls showed focal perineuronal dot-like pattern and 3 cases of GBM showed focal axonal and nuclear staining in adjacent normal brain tissue. Endothelial cell staining for IMP3 was found in 1 of 21 cases (4.8%) of PA, 15 of 38 cases (39.5%) of GBM, and 6 of 18 cases (33.3%) of recurrent GBM, and the difference between PA and GBM was statistically significant ($p=0.005$). In 1 case of GBM, IMP3 highlighted an arcade vasculature pattern but the tumor cells were completely negative. Surprisingly, of the 18 recurrent GBM cases, 5 showed IMP3 negativity in the initial tumor and positivity in the recurrence. In contrast, 4 cases showed IMP3 positivity in initial tumors but negativity in recurrences. The mean IMP3 staining intensity in positive cases was 2.5+ in PA, 2.9+ in GBM, and 2.4+ in recurrent GBM, and the difference between GBM and recurrent GBM was statistically significant ($p=0.0336$).

Conclusions: The presence of a higher level of IMP3 in tumor cells and associated endothelial cells in GBM compared to PA supports that IMP3 may be useful in differentiating PA from GBM in small biopsy specimens. Recurrent GBM shows similar IMP3 expression to GBM but with lower staining intensity. The significance of IMP3 expression in endothelial cells in GBM is unclear.

1810 aPKC-Dependent EGFR and NF- κ B Signaling Co-Operate To Promote Glioblastoma Invasion

AS Perry, Y Kusne, M Jabbar, E Mandell, W McDonough, K Aldape, ME Berens, JC Loftus, EJ Rushing, S Ghosh. Brigham and Women's Hospital, Boston, MA; Barrow Neurological Institute/St. Joseph's Hospital, Phoenix, AZ; Arizona State University, Tempe, AZ; The University of Arizona, Tucson, AZ; Translational Genomics Research Institute, Phoenix, AZ; MD Anderson Cancer Center, Houston, TX; Mayo Clinic Arizona, Scottsdale, AZ; Armed Forces Institute of Pathology, Washington, DC.

Background: Glioblastoma multiforme (GBM) is the most common primary brain tumor with an average untreated survival of three months and 14 months with therapy. Successful anti-EGFR targeted therapy has proven elusive despite profound success in other tumors and clear pathogenesis in GBM. This resistance may be due to shunting of tumor signaling. We present evidence of EGFR kinase inhibitor resistance through activation of NF- κ B signaling, mediated by the protein kinase aPKC.

Design: Using a co-culture model of human GBM cells and macrophages, we measured GBM invasion with NF- κ B and EGFR signaling modulators. In vivo testing included demonstration of activity in human GBM tissue arrays and patient survival was compared by the cox hazard ratio between aPKC, EGFR groups.

Results: Anti-TNF- α antibody or inhibition of NF- κ B signaling within GBM cells attenuates invasion of GBM in an EGFR-independent manner. Upon co-culture of GBM cells with macrophages, autocrine production of TNF- α and NF- κ B signaling is increased. This was dependent on protein kinase aPKC association with scaffold proteins regulating the TNF- α dependent transcription of IL-1 β , IL-8, TNF- α and MCP-1. The aPKC-Par6 complex also regulated EGF-dependent Rac activation, transcription of a number of EGF-dependent invasion-associated genes (CD44, VCAM, MMP9, uPAR), and the actin cytoskeleton. It was found that aPKC bridges both EGFR and NF- κ B pathways in GBM. Silencing of aPKC was more effective in inhibiting GBM invasion, particularly under GBM cell-macrophage co-culture conditions. High activity of aPKC was shown in GBM tissue arrays with a significant correlation between macrophage/microglial infiltration, aPKC and poor GBM survival independent of EGFR expression.

Conclusions: In conclusion, macrophage derived TNF- α activates NF- κ B signaling and was found to confer resistance to EGFR kinase inhibitors through aPKC. The protein kinase aPKC is a critical component of both EGFR and NF- κ B signaling pathways in GBM cells and may be an attractive therapeutic target for future studies.

1811 Utility of Whole Genome Amplification (WGA) To Enable Virtual Karyotyping with SNP Arrays in Paraffin-Embedded Brain Tumor Biopsies with Limited Tissue

S Pina-Oviedo, K Alvarez, SZ Powell, CC Chang, FA Monzon. The Methodist Hospital, Houston, TX.

Background: Virtual karyotyping with SNP (single nucleotide polymorphism) arrays has been established as a novel and reliable diagnostic tool for several types of tumors, including brain tumors. Specific molecular alterations have been linked to central nervous system (CNS) neoplasms, such as co-deletion of 1p19q in oligodendrogliomas and overexpression of *EGFR* in glioblastomas. Frequently, very small samples are obtained from brain biopsies and the limited amount of tissue may limit the ability to obtain an accurate diagnosis. We evaluated the use of whole genome amplification (WGA) in order to perform virtual karyotyping in paraffin-embedded brain tissue biopsies.

Design: DNA was extracted from microdissected tissue from paraffin-embedded blocks in three cases of oligodendrogliomas and one case of glioblastoma that were confirmed by morphology and evaluated for 1p/19q deletions by fluorescence in-situ hybridization (FISH). WGA of extracted DNA was performed using the RepliG FFPE kit (Qiagen) with manufacturer's recommendation and with a modified protocol. Virtual karyotyping was then performed on these samples using Affymetrix 250K *Nsp* SNP arrays. Additional tumor samples from other tissue types were also evaluated to evaluate the reliability of the method.

Results: By using WGA with SNP arrays we were able to confirm the presence of 1p19q co-deletion starting from 50ng of DNA from the anaplastic oligodendroglioma and glioma samples. In addition, characteristic chromosomal imbalances were identified in the glioblastoma including amplification of *EGFR*. Our results correlated with the results obtained from FISH in all cases. The WGA method was successfully applied to samples from kidney and bone marrow specimens.

Conclusions: We demonstrate that whole genome molecular analysis tools can be used in samples with limited amount of tissue by using WGA and SNP cytogenomic arrays. Our data demonstrates that WGA can be potentially used as a diagnostic tool in small samples, especially those where diagnosis cannot be established on routine grounds but further testing is hampered by the limited amount of tissue. Although the efficacy our WGA approach was of 100% of the cases, larger series are necessary to confirm the reliability of this method. This technique should be of practical use in neuropathology, since frequently CNS biopsies are small and molecular analysis are increasingly used to confirm diagnoses and for selection of therapy.

1812 Pilocytic Astrocytomas of the Optic Nerve and Their Relation to Pilocytic Astrocytomas Elsewhere in the Central Nervous System

GF Reis, M Bloomer, A Karnezis, J Phillips, P Goldhoff, T Tihan. University of California San Francisco, San Francisco, CA.

Background: Pilocytic astrocytoma (PA) is an indolent neoplasm common in children. Total resection typically provides cure, but many PAs cannot be totally resected and require adjuvant treatment. PA of the optic nerve (a.k.a. optic glioma) is a subtype with more aggressive behavior. In most studies, these have been considered within a larger category of "optic pathway glioma" that included hypothalamic PAs. BRAF gene duplication and activation of downstream MEK/ERK has been recently reported in PA, but very few to no optic nerve tumors were evaluated. Our study reviews the clinicopathological and molecular features of optic nerve PAs to determine whether they can be distinguished from PAs located elsewhere in the central nervous system (CNS). **Design:** We searched for optic PAs treated at the University of California Medical Center (UCSF) between 1954-2010. In addition, we utilized data from a recent multi-institutional study of intracranial PA for comparison. Clinical information was obtained from medical records, and cases were selected based on histologic diagnosis. We assessed BRAF duplication by immunohistochemistry and FISH. Immunohistochemistry included standard markers as well as p16, phospho-histone H2AX, and pERK.

Results: We identified 22 patients (16 male, 6 female) with optic nerve glioma. The median age of diagnosis was 9 years. All patients underwent surgery, and gross total resection was achieved in 15 cases. One patient received chemotherapy; none received radiation. There were no deaths. When compared to intracranial PA, there was no statistical significance in terms of median age ($P = 0.21$). Post-surgical treatment was significantly different in terms of radiotherapy and chemotherapy. While the follow-up was longer and more complete for the intracranial group, differences in outcome were noted between the groups. Immunohistochemistry for BRAF was not useful in determining BRAF duplication, but FISH analysis showed that BRAF duplication was more frequent in posterior fossa PA ($p < 0.001$). Staining for p16 was more frequently observed in tumors with BRAF duplication. H2AX staining was not useful in distinguishing among PA subtypes.

Conclusions: The strong correlation between BRAF duplication and pERK/p16 positivity suggests that the BRAF/p16 pathway is active in a subset of PAs and may be associated with oncogene-induced senescence. Our study further supports the increasing body of evidence suggesting that BRAF duplication is more typical of posterior fossa PA and is distinctly less common at other sites.

1813 AEG-1 Gene Copy Number Alterations in Human Gliomas

HT Richard, JF Harrison, GN Fuller, PB Fisher, CE Fuller. Virginia Commonwealth University, Richmond, VA; University of Texas-MD Anderson, Houston, TX.

Background: Gliomas represent the most common primary brain tumors in all age groups. Over the past few decades, research has uncovered numerous molecular alterations and pathway dysregulations involved in gliomagenesis. Although many potential biomarkers have been identified, treatment options for gliomas are limited, and mortality remains unacceptably high. Astrocyte elevated gene-1 (AEG-1) is a transmembrane protein that modulates multiple signal transduction pathways. AEG-1 overexpression has been found in cell lines and patient-derived samples of various carcinomas, neuroblastoma, and melanoma; *AEG-1* gene amplification has similarly been found in breast and liver carcinomas. High AEG-1 expression was found in >90% of brain tumors in a recent study, particularly malignant gliomas. The current study aims to determine the incidence of *AEG-1* gene copy number alterations in a broad cohort of gliomas.

Design: We reviewed the histologic features of 190 gliomas from two institutions. Dual color fluorescence in situ hybridization (FISH) was performed on tissue microarrays containing tumor core samples. A locus-specific probe targeting *AEG-1*(8q22) was paired with control probe for the centromeric region of chromosome 8 (CEP8). Correlations were sought between pathologic parameters and gene copy number status. Low level gain was defined as an *AEG-1*/CEP8 ratio of 1.2-2.0, with gene amplification having a ratio >2.0.

Results: The cohort included 81 glioblastoma / gliosarcoma (G), 27 anaplastic astrocytoma (AA), 17 anaplastic oligodendroglioma, 14 anaplastic oligoastrocytoma, 2 grade II astrocytoma, 21 oligodendroglioma, 8 oligoastrocytoma, 2 pleomorphic xanthoastrocytoma, 16 pilocytic astrocytoma (PA), and 2 glioneuronal tumors. Overall, 21% of gliomas tested harbored *AEG-1* copy number gains. Gains were more frequently encountered in oligoastrocytomas (31%), AA (37%), and G (19%), though 13% of oligodendrogliomas were similarly involved. The majority of copy number alterations

were low level gains, though 8% represented *AEG-1* amplifications; the later finding was limited to high grade astrocytomas (AA and G). Of note, 12.5% of PA had *AEG-1* copy number gain, whereas all other low grade gliomas were negative.

Conclusions: *AEG-1* gene copy number gains are present in a wide variety of infiltrative gliomas as well as PA. Further basic science and translational studies will be needed to clarify AEG-1's viability as a prognostic biomarker and/or therapeutic target in gliomas.

1814 Impact of Oncogenic Alterations on MGMT Promoter Methylation Status in Glioblastoma (GBM)

Y Rong, C Vincentelli, C Chisolm, JJ Olson, C Hao, SB Hunter, DJ Brat. Emory University School of Medicine, Atlanta, GA.

Background: GBM is the most common primary malignant brain tumor and consists of multiple genetic subtypes. *O*⁶-methylguanine – DNA methyltransferase (MGMT) is a key DNA repair enzyme that antagonizes chemotherapy-induced DNA crosslinking at the *O*⁶ position of guanine. *MGMT* promoter methylation, found in ~ 40% GBMs, is associated with reduced MGMT expression, enhanced response to temozolomide and improved survival. Here we investigate correlations between specific genetic alterations and *MGMT* promoter methylation in GBM.

Design: Results of molecular testing on 120 primary GBMs diagnosed from 2008 to 2010 at Emory University were analyzed. Methylation of the *MGMT* promoter was determined by methylation-specific PCR. *EGFR* amplification (amp) and *PTEN* deletion (del) were detected by fluorescence in situ hybridization (FISH). Immunohistochemistry was used to detect mutant IDH1 expression (IDH1R132H).

Results: Among GBMs in this study, *MGMT* promoter methylation was detected in 55 of 120 (46%); *EGFR* amp in 45 of 120 (38%); *PTEN* del in 72 of 78 (92%); both *EGFR* amp and *PTEN* del in 27 of 73 (37%); and IDH1 mutation in 13 of 109 (12%). *MGMT* promoter methylation was present in 25 of 45 (56%) cases with *EGFR* amp and in 25 of 75 (33%) with wt *EGFR* (Fisher's exact test, $p < 0.05$); 34 of 72 cases (47%) with *PTEN* loss and in 3 of 6 (50%) with *PTEN* intact; and in 19 of 27 (70%) with both *EGFR* amplification and *PTEN* loss ($p < 0.05$). *MGMT* promoter methylation was present in 9 of 13 (69%) cases with mutant IDH1 protein detected and in 44 of 96 (46%) without mutant IDH1 detected ($p = 0.1$).

Conclusions: Our results indicate that *MGMT* promoter methylation is most frequent in those GBMs with *EGFR* amplification and *IDH1* mutation.

1815 BRAF V600E Mutation Is Seen in 50% of Adult Pleomorphic Xanthoastrocytoma with Anaplastic Features but Does Not Predict Prognosis for Individual Patients

YX Schmidt, BK Kleinschmidt-DeMasters, DL Aisner, KO Lillehei, D Damek. University of Colorado Denver SOM, Aurora, CO.

Background: Pleomorphic xanthoastrocytoma with anaplastic features (PXA-A) is an uncommon tumor about which little is known regarding prognostic factors. Indeed, debate exists as to which histological features (number of mitoses, MIB-1 rate, necroses) best correlate with anaplasia in this tumor type. PXAs often have *BRAF V600E* mutation, although the actual percentage of + cases is variable. Dias-Santagata *et al.* found 60% of PXAs WHO grade II and 17% of PXA-As + for mutation, whereas Schindler *et al.* identified mutation in 63-69% of PXAs WHO grade II and 38% of adult PXA-As and 100% of pediatric PXA-As. It is unknown if the mutation has value for predicting individual patient outcome. In addition, virtually no information exists about immunohistochemistry for IDH-1 in PXA-A.

Design: Eleven cases of adult PXA-A were reviewed. Ten cases were assessed for the *BRAF V600E* mutation by PCR and ten for IDH-1 by IHC.

Results: Patients ranged in age from 18-68 years; 5/11 PXA-As affected temporal lobe and 2/11 tumors were cystic. 5/11 had gross total resection; all but 2 received external beam cranial irradiation; 10/11 received adjuvant chemotherapy (TMZ, BCNU). A dichotomy existed for survival: 4 survived less than 2 years. Long term survivors, in contrast, are alive at 7, 9.3, 10.9, and 11.4 years post diagnosis. Of these long term survivors, only 2 of 4 manifested *BRAF V600E* mutation. Interestingly, these two patients were amongst the youngest ages in the cohort, at 18 and 28 years. Another young patient (22 years) did possess the *BRAF V600E* mutation, but succumbed to his disease 1.7 years after diagnosis; he received only subtotal resection and was the single patient who refused post-operative chemo- or radiotherapy, underscoring the need for adjuvant treatment. Correlating with the series by Schindler *et al.* that suggest higher incidence of *BRAF* mutation in pediatric versus adult PXA-As, in our series, 3 of 4 patients over age 45 years were negative; a 68-year-old did show *BRAF* mutation; her survival after diagnosis was 1.9 years. Almost all patients were negative for IDH-1 immunoreactivity.

Conclusions: *V600E BRAF* mutation is seen in at least 50% of PXA-As in adults; mutational status has no positive or negative predictive value for individual patients in terms of survival. Positive mutation is not exclusive to younger-aged individuals. Negative IDH-1 by IHC is usually identified in PXA-As of adults.

1816 Natalizumab-Associated T Cell Complications: First Case of Peripheral T Cell Lymphoma and Second Case with PML-IRIS and Clonal T Cell Production

JT Schowinsky, JR Corboy, TL Vollmer, BK Kleinschmidt-DeMasters. U. Colorado SOM, Aurora, CO.

Background: Natalizumab (NTZ) is a therapeutic monoclonal antibody approved in 2004 for treatment of patients with the relapsing form of multiple sclerosis (MS). NTZ reduces MS relapses as well as new inflammatory lesions on MRI and has significant clinical efficacy. Unfortunately, soon after approval, occurrence of progressive multifocal leukoencephalopathy (PML) due to reactivation of JC virus infection in oligodendrocytes was associated with use of NTZ (Kleinschmidt-DeMasters, Langer-Gould), and NTZ was temporarily removed from the market. Availability resumed in

2006 with monitoring programs, including serological testing for JC virus exposure. To date, >80,000 patients with MS have used NTZ and despite cautious use, PML cases continue to be reported. In patients with PML after NTZ withdrawal, an immune reconstitution inflammatory syndrome (IRIS) can occur, a condition for which there is limited histological information, particularly with long-standing IRIS and particularly at autopsy. Only a single case of lymphoma has previously been reported as a complication of NTZ (primary CNS B cell).

Design: We report two MS patients with NTZ use who developed T cell abnormalities. **Results:** The first is a 39yo woman who developed a symptomatic skull mass in 2010 that proved to be peripheral T cell lymphoma, NOS (CD3+, CD4-, CD8-). Subsequent marrow and vertebral body biopsies have remained positive despite aggressive therapy; she remains alive but doing poorly. The second patient was a 56yo woman with relapsing remitting MS, treated for 4 years with NTZ, who discontinued drug in the summer of 2010 after diagnosis of PML. CSF analysis in November 2010 showed normal results by flow cytometry and cytology; CSF protein was 50 mg/dl; with 26 WBCs: 91% lymphocytes, 9% monocytes. JC virus was <100 and HHV-6 <250. PML versus IRIS was diagnosed; comfort care was instituted but demise did not occur until a year after NTZ withdrawal. Autopsy showed massive cavitory brain lesions far more destructive than with previously reported PML-natalizumab or PML-IRIS cases, with abundant perivascular and parenchymal CD8+ T cell infiltrates; Monoclonal T cell populations were detected in both marrow and spleen, suggesting emergence of a pre-lymphomatous population, but no overt lymphoma was seen histologically. We interpret this case as prolonged severe PML-IRIS with overstimulation of T cells.

Conclusions: Complications of NTZ have largely been centered on PML, but these two cases suggest T cell abnormalities can occur. We report the first example of peripheral T cell lymphoma with NTZ use.

1817 Gliomas Arising in Patients with Multiple Sclerosis Have No Distinctive Genetic Features

HS Serracino, A Khalil, D Damek, D Ney, KO Lillehei, BK Kleinschmidt-DeMasters. University of Colorado at Denver, Aurora, CO.

Background: The co-occurrence of gliomas and multiple sclerosis (MS) in the same patient is uncommon, but a well-reported phenomenon, with 39 cases in the literature since 1980. One-third of these gliomas have been glioblastomas (GBMs), although oligodendrogliomas and astrocytomas, WHO grade II and III, have also been reported. In most cases, the glioma has developed many years after the diagnosis of MS, leading authors to postulate that chronic inflammation and chronic gliosis in demyelinating plaques is the underlying substrate for secondary induction of a glial neoplasm. Until recently, however, additional molecular or genetic tools have not been available to test the hypothesis as to whether high-grade gliomas might arise from chronic gliosis, with transformation to low grade glioma, and eventually GBM, i.e., be secondary GBMs.

Design: We utilized text word searches of our databases to identify MS-gliomas and assessed for the first time all MS-GBMs for immunohistochemical (IHC) and genetic markers more frequently associated with secondary than primary GBMs, namely IDH-1 and p53 IHC, as well as for LOH 10q (PTEN locus) and EGFR amplification, two features more characteristic of primary than secondary GBM. The eight cases identified (5 males: 3 females) represent the second largest series of MS-gliomas in the literature and include a tumor type not previously reported, an incidental pilocytic astrocytoma of midbrain identified at autopsy. This represented the only autopsy case in >175 MS brains in our Rocky Mountain MS Tissue Bank. The mean and median age at glioma diagnosis for our cases was 45.4 and 49 years for men, and 49 and 41 years for women, respectively. These numbers are comparable to mean and median age at glioma diagnosis previously reported in the literature: 49.06 and 47.5 years for men and 45.38 and 44.5 years for women, respectively.

Results: None of the 4/8 GBMs showed IDH-1 + IHC and no distinctive pattern was detectable for PTEN loss or EGFR amplification. Only 1/4 GBMs had nuclear p53 IHC in greater than 90% of the cells.

Conclusions: Our genetic data, when taken together with epidemiological data from our MS Brain Bank, shows no strong prevalence of gliomas in MS patients and further argues against the hypothesis that gliosis in MS predisposes to glioma formation, i.e., secondary GBMs.

1818 Cavernous Angiomas in Chronic Epilepsy Associated with Focal Cortical Dysplasia

ER Severson, DJ Chen, RA Prayson. Cleveland Clinic, Cleveland, OH.

Background: Both cavernous angiomas and focal cortical dysplasia (FCD) are well recognized causes of medically intractable epilepsy. In a subset of patients with chronic epilepsy, multiple pathologies may coexist (eg: focal cortical dysplasia adjacent to ganglioglioma or dysembryoplastic neuroepithelial tumor). Anecdotal causes of FCD adjacent to cavernous angiomas have been documented in the literature. This study systematically reviews a series of cavernous angiomas in epileptic patients, looking for evidence of coexistent FCD.

Design: One hundred forty six patients were diagnosed with cavernous angiomas on resection specimens from January, 1989, to May, 2011. Histologic slides were reviewed from these cases in order to confirm the diagnosis and to identify cases which had ample tissue adjacent to the lesion to evaluate for FCD. Eighteen cases who also had epilepsy qualified for study. FCD was classified according to criteria outlined by Palmini et al (Neurology 2004;62(Suppl 3)S2-8).

Results: Patients included 10 females (55.6%) and 8 males (44.4%) with a mean age of 38.5 years (median 39 years; range 21 to 51 years) at the time of resection. All patients had a history of epilepsy (median 11 years) prior to surgery. Seventeen cavernomas were located in the temporal lobe and one in the occipital lobe; 9 were located on the left side and 9 on the right side. Adjacent FCD was identified in 13 out of the 18 cases

(72.2%). The FCD in these cases were classified as type Ia (N=8; 61.5%), type Ib (N=4; 30.8%), and type IIa (N=1; 7.7%). After resection, a majority of the patients experienced resolution of epilepsy (N=14; 77.8%). Of the four patients that did not experience resolution, 2 had evidence of adjacent FCD (type Ia = 1, type Ib = 1) and 2 did not.

Conclusions: Focal cortical dysplasia is frequently present in association with cavernous angiomas in patients with chronic epilepsy. The type of FCD seen adjacent to these lesions vary, but most are Palmini et al type I. With resection of the cavernous angiomas and adjacent FCD, resolution of epilepsy may be achieved.

1819 Therapeutic Combination of Novel Mitochondrial Hsp90 Inhibitors, Gamitrinibs, with Phosphatidylinositol 3-Kinase Inhibitors Exerts Therapeutic Activity Against Glioblastoma In Vivo and In Vitro without Significant Toxicity

MD Siegelin, DC Altieri. Columbia University College of Physicians & Surgeons, New York, NY; The Wistar Institute Cancer Center, Philadelphia, PA.

Background: The identification of novel effective treatment strategies for glioblastoma WHO IV remains a challenge. Recent data demonstrated that Heat-shock-protein 90 (Hsp90) is preferentially over-expressed in tumor mitochondria. Gamitrinibs are a novel class of Hsp90 inhibitors that inhibit mitochondrial Hsp90 activity. As many primary glioblastomas harbor well characterized genetic alterations of molecules of the phosphatidylinositol 3-kinase (PI3-Kinase) pathway, a combinatorial targeted approach of the PI3-kinase and mitochondrial Hsp90 might be a worthwhile treatment strategy for high-grade gliomas.

Design: Glioma cell lines were treated with Gamitrinibs, PI3-Kinase inhibitors or the combination of both. Apoptosis and caspase-activity were analysed by Annexin V/PI staining and immunoblotting, respectively. U87 glioblastoma cells stably transfected with a luciferase expression plasmid were stereotactically intracranially implanted in the right striatum of nude mice. Animals with established tumors were randomized in 4 groups (4 animals/group) and started on sterile vehicle (cremophor), Gamitrinib, NVP-BEZ235 (PI3-Kinase inhibitor), or the combination of Gamitrinib-G4 and NVP-BEZ235.

Results: The combination of PI3-kinase inhibitors with suboptimal dosages of Gamitrinibs resulted in rapid apoptosis induction in glioblastoma cells. Mechanistically, the combination treatment enhanced the activation of caspases. Similarly vector-driven forced expression of a dominant negative PI3-Kinase construct in U251 glioma cells sensitized glioblastoma cells to Gamitrinib mediated apoptosis. Moreover, in an orthotopic intracranial xenograft mouse model the combination of Gamitrinib-G4 with NVP-BEZ235 (PI3-Kinase inhibitor) significantly reduced proliferation of tumor cells and significantly extended animal survival in the combination group (Gamitrinib+NVP-BEZ235) as compared to vehicle-treated, Gamitrinib-G4 and NVP-BEZ235 single treated animals. Most important, the combination of Gamitrinib and NVP-BEZ235 did not reveal significant signs of toxicity in vivo.

Conclusions: Gamitrinibs are powerful mitochondrial Hsp90 inhibitors that in combination with PI3-Kinase inhibitors reveal significant anti-glioma activity both in vitro and in vivo.

1820 Evaluation of Interactions of PI3K Pathway, IDH1(R132H), and OLIG2 Expression in Newly Diagnosed Glioblastoma Clinical Outcomes

S Sioletic, B Alexander, L Lauriola, M Balducci, K Ligon. Dana Farber Cancer Institute, Boston, MA; Gemelli Hospital, Rome, Italy.

Background: Clinical trial design for evaluation of emerging PI3K pathway inhibitors in glioblastoma (GBM) has generally focused on stratification of patients using biomarkers of PI3K pathway status but have not attempted to control for known heterogeneous survival in subtypes of glioblastoma which may significantly affect/distort correlation of outcomes with PI3K biomarkers. In particular, the IDH1 (R132H) mutation and OLIG2 expression levels are proposed to help identify gliomas with prolonged survival and sensitivity to conventional treatment. We evaluated a well-defined cohort of GBM for PI3K pathway activation and status of IDH1(R132H) mutation and OLIG2 expression in primary GBM and correlate with the clinical outcome of the patients.

Design: A total of 82 patients (M/F 43/39; median age: 56; range: 21-78) who had undergone surgical resection for newly diagnosed glioblastoma were pathologically re-reviewed and used to construct a tissue microarray. All subjects had undergone a full course of conventional fractionated radiotherapy (RT) and temozolomide. Tissue microarray sections were IHC stained and scored manually for OLIG2, Ki67, TP53, IDH1(R132H), PTEN, and pAKT-473.

Results: Clinical follow-up was available for all the patients (median: 27 months; range: 5-81 months). IDH1(R132H) was positive in 5 cases (6%) with a median survival of 49 months (3 patients alive). OLIG2 was positive in at least 60% of tumor cells in 32 patients (43%), no GBM with more than 90% of OLIG2 positive cells was found. 28 of the patients with OLIG2+/IDH1(R132H)- had a median survival of 22 months. pAKT staining was positive (>60% of the cells) in 59 patients (71%). Evidence for complete PTEN protein loss was found in 7 patients (8%). In our cohort only 6 patients (7%) showed a 2+ score similar to vessel staining. A positive correlation of high PTEN expression (2+) and pAKT (>80% of the cells) has been detected. PTEN loss (score 0) significantly correlated with progression following treatment (PD) (85% vs. 48% of all GBM). PTEN 2+, showed a significant response (all except one with PD), had a clinical responses (CR) (83% vs. 32% of all GBM) after RT and CT, however the overall survival did not change.

Conclusions: Of all the markers studied only IDH1(R132H) and Olig2 were found to be independent positive prognostic markers. PTEN, although doesn't have any predictive value in the conventional treatment of GBM, when is lost or overexpressed can be used to identify the patients that can have a clinical response to temozolomide.

1821 Gene Expression Profiling on Matched Neurofibroma/MPNST Pairs

T Stricker, K Henriksen, A Montag, T Krausz, P Pytel. University of Chicago, Chicago, IL.

Background: In the setting of neurofibromatosis type 1 (NF1) a clear malignant transformation from preexisting benign neurofibroma into malignant peripheral nerve sheath tumor (MPNST) is well documented. In NF1 these tumors therefore allow the study of biologic factors important for this malignant transformation.

Design: We selected 12 cases of MPNSTs arising within pre-existing plexiform neurofibromas. For each case RNA was isolated from formalin fixed paraffin embedded neurofibroma and the matched MPNST. The resulting 24 samples were used to analyze the expression of 519 kinase genes using Nanostring nCounter technology. Expression was normalized across samples using a generalized linear model framework, and the log 2 transformed residuals from this model were used for subsequent analysis. Differentially expressed kinases between neurofibromas and MPNSTs as a group were assessed by Wilcoxon test, followed by correction for multiple testing using false discovery rate. Differential expression between NF and MPNST within an individual was assessed by fold change.

Results: Principle component analysis of kinase expression demonstrates that differential expression of kinase genes is sufficient to separate most of MPNSTs from neurofibromas. Interestingly, two of the MPNSTs clustered more closely with neurofibromas than the remaining MPNSTs despite the fact that their histology was not low-grade. The neurofibromas formed a much tighter cluster, while MPNSTs were more heterogeneous. 135 genes were differentially expressed at a FDR of 5%. Pathway analysis of differentially expressed genes shows that kinases involved in MAP kinase signaling pathways and kinases involved in the cell cycle, including cyclin dependent kinases and gene involved in chromosomal segregation are upregulated in MPNSTs. Genes that were differentially expressed between neurofibroma and MPNST from the same individual were identified by ranking fold changes. Although there was extensive diversity in these lists, reflecting the diversity of MPNSTs, a few common genes were apparent. The most common upregulated gene was NTRK1, which was upregulated in 9/12 MPNSTs.

Conclusions: In the performed analysis neurofibromas are relatively similar in their expression patterns while MPNSTs exhibit significant diversity. This diversity suggests that even MPNSTs arising in the well defined setting of a plexiform neurofibroma in NF1 are still a quite heterogeneous group of tumors. Components of the MAP kinase signaling pathway, NTRK1 and factors involved in chromosomal segregation were upregulated in MPNSTs.

1822 An Autopsy Study of Fatal Febrile Encephalopathy

RK Vasishta, S Kumar, N Kakkar, K Gupta, A Bhalla, PD Singhi. Post Graduate Institute of Medical Education and Research, Chandigarh, UT, India.

Background: Febrile encephalopathy is a term used to denote patients presenting with fever and altered mentation. It is a common condition leading to emergency admissions in both adults and children in India. The profile of acute febrile encephalopathy varies across different geographic regions with newer agents being increasingly recognized all over the world. This study is aimed at knowing the etiology in fatal cases presenting clinically as "febrile encephalopathy".

Design: All adult and pediatric cases autopsied in the Department of Histopathology, PGIMER with the clinical diagnosis of febrile encephalopathy over a period of 14 years (1996-2010) were analyzed.

Results: A total of 80 autopsy cases were analyzed. Viral encephalitis (41/80 cases i.e. 51%) was the commonest cause of febrile encephalopathy with Japanese encephalitis accounting for 65.8% (27 of 41 cases) of all viral encephalitis in this study. This was followed by bacterial meningitis in 10 cases (13%) of which 7 were tubercular and 3 pyogenic. Other causes documented were cerebral venous thrombosis (3), cerebral malaria (2), acute haemorrhagic leucoencephalitis (2), primary amoebic meningoencephalitis (1) and Leigh's syndrome (1). Non specific changes were seen in 20/80 i.e. in 25 % of the cases.

Conclusions: Viral encephalitis of which majority of cases were of Japanese encephalitis is the commonest cause of febrile encephalopathy in this study. Non specific changes are seen in a substantial number i.e. 25 % of the cases of febrile encephalopathy.

1823 Survival Benefit of Temozolomide as Treatment for Glioblastoma; a Population Based Analysis

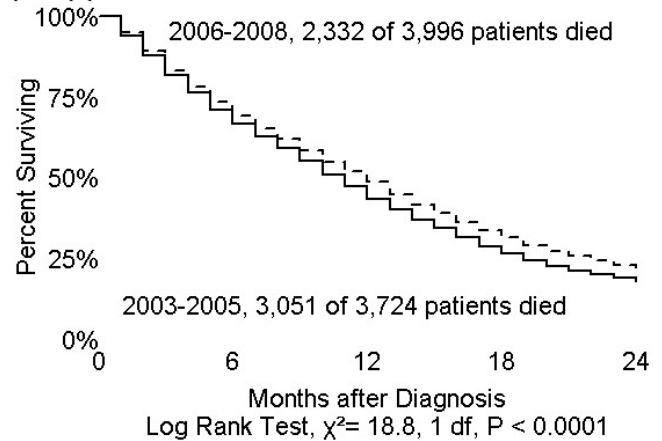
MS Wachtel, BB Miller. Texas Tech University Health Sciences Center, Lubbock, TX.

Background: In 2005, the European Organisation for Research and Treatment of Cancer Brain Tumor and Radiotherapy Groups and the National Cancer Institute of Canada Clinical Trials Group reported improved survival after diagnosis of glioblastoma multiforme when temozolomide was administered with radiotherapy versus treatment by radiotherapy alone. Hypothesized was the notion that a large database might identify improved survival in patients diagnosed with glioblastoma multiforme since publication of that study.

Design: A case listing session of the Surveillance, Epidemiology, and End Results Program of the National Cancer Institute was performed to retrieve data concerning persons 40-70 years old at histologic diagnosis of glioblastoma multiforme for the periods 2003-2005 and 2006-2008 who had survived at least one month. Race, gender, age, and survival times were acquired. Two-year survival experiences were compared. Survival estimates were calculated by the Kaplan-Meier procedure. Log normal accelerated failure time regression estimated survival time ratios; the 2.5th and 97.5th percentiles of 3,000 bootstrap replicates were calculated to provision 95% confidence intervals. Age was transformed by a natural spline with five knots before entry into regression.

Results: The median age at diagnosis for the 7,720 patients was 58 years (interquartile range 52-64 years). 6960 (90.2%) were White, 412 (5.3%) were Black, and 348 (4.5%) were of unknown/other race. 3,030 (39.2%) were women; 4,690 (60.8%) were men. The figure displays survival curves. Adjusted for age, gender, and race, survival times for 2006-2008 were 11.4% (95% confidence interval 5.7-17.5%) longer than for 2003-2005.

Conclusions: Patients diagnosed after 2005 lived longer. Benefits of temozolomide in the treatment of glioblastoma multiforme are supported by analysis of the general patient population.



1824 Fully Automated Dual ISH (Dual-Color Dual-Hapten Silver In Situ Hybridization) for + Amplification in Glioblastomas

Z Wang, B Portier, C Lanigan, RR Tubbs. Cleveland Clinic, Cleveland, OH.

Background: *EGFR* amplification occurs in 40-60% of primary glioblastomas and is typically detected by fluorescence *in situ* hybridization (FISH). In this study, detection of *EGFR* amplification by automated dual-color dual-hapten silver ISH (DDISH) was compared to FISH in a series of 73 glioblastomas.

Design: FISH testing was performed on paraffin embedded formalin fixed tissue using a commercially available *EGFR* ASR probe paired with a CEP7 centromeric control probe (Abbott Molecular). In addition to FISH each case was analyzed independently by DDISH. DDISH staining was performed using the Dual Color Open Probe software on a Ventana Benchmark XT. DNP labeled/repeat depleted *EGFR* and Digoxigenin labeled Chromosome 7 (CHR7) probes were utilized. Pretreatment conditions were: Extended II deparaffinization at 72°C, 3 cycles of cell conditioning with CC2 for 12 minutes at 80°C, and protease digestion with ISH protease 3 for 32 minutes. Denaturation was at 80°C for 12 minutes; hybridization at 44°C for 6 hours; followed by stringency washes (3 at 72°C, 8 minutes). *EGFR* DNP probe was detected with ultraView silver ISH (SISH) DNP Detection Kit: silver anti-hapten antibody (20 minutes), and SISH detection (8 minutes). CHR7 DIG probe was detected with ultraView Red ISH DIG Detection Kit: anti-hapten antibody incubated (20 minutes) and Red detection (8 minutes). The slides were counterstained with hematoxylin II for 8 minutes, post counterstained with bluing reagent for 4 minutes, and mounted as permanent slides for bright field microscopy. Metallic black silver (*EGFR*) and reference CHR7 red signals were qualitatively and semi-quantitatively enumerated for tumor nuclei. Small and large clusters of silver signals were recorded as 6 or 12 signals respectively. *EGFR* amplification was defined as *EGFR*/CHR7 ratio >2.0.

Results: Evaluable signals with amplified (n=29) and non-amplified (n=40) DDISH were obtained in 69 cases (95%). Concordance between FISH and DDISH was observed for all cases. FISH-defined *EGFR* counts (mean 17.4 vs. 2.7) and *EGFR*/CEP7 ratios (mean 6.0 vs. 1.1) for DDISH amplified and DDISH non-amplified cases were significantly different (p<0.0001).

Conclusions: In this representative series of glioblastomas, utilization of DDISH correctly identified all *EGFR* amplified cases as previously assessed by FISH. These data suggest that DDISH can be utilized as an ancillary tool for detecting *EGFR* amplification and therefore may be useful in molecular characterization of gliomas.

1825 Quantitative Analysis of MGMT Promoter Methylation in Glioblastoma Multiforme

B Yang, R Read, R Tubbs. Cleveland Clinic, Cleveland, OH.

Background: O⁶-Methylguanine-DNA methyltransferase (MGMT) is a DNA repair enzyme that specifically removes alkyl groups from the O⁶ position of guanine in DNA. Repair of O⁶-alkylguanine adducts by tumour cells has been implicated in drug resistance since it reduces the cytotoxicity of alkylating chemotherapeutic agents. Recent clinical trial reveals that glioblastoma patients with MGMT methylation had much better response to temozolomide and median survival nearly doubled than those without MGMT methylation. In order to provide this molecular biomarker in guidance of chemosensitivity, we have developed and validated MGMT methylation assay using pyrosequencing on small biopsy specimens of glioblastoma multiforme.

Design: Promoter methylation of MGMT was quantitatively analyzed in 43 cases of glioblastoma multiforme and 10 cases of non-neoplastic epilepsy brain tissue. MGMT methylation profile is analyzed quantitatively using Pyro Q96 on paraffin-embedded biopsy tissues. The analytical sensitivity and minimal requirement of DNA volume and biopsy size is evaluated. Two cell lines, one harboring of MGMT methylation and another free of MGMT methylation were included as positive and negative controls. The sensitivity between pyrosequencing and methylation-specific PCR was also compared.

Results: Using a cutoff at 10%, methylation of MGMT was identified in 33% (11/33) cases of glioblastoma and 0% of the non-neoplastic epilepsy brain tissue. The range of percentage of methylation of any CpG island in MGMT promoter is 33-95% with a mean of 65%. By a series dilution of a methylated cancer cell line with an unmethylated normal cell line, pyrosequencing can detect 5% of tumor cells harboring MGMT methylation. The minimal amount of genomic DNA required to be able to successfully detect MGMT methylation by pyrosequencing is at 100 ng (approximately 3,000 cells). In comparison with MSP, pyrosequencing is comparably sensitive with less false-positive cases and also provide quantitative methylation value of each CpG island.

Conclusions: We have studied and validated the quantitative MGMT methylation assay on small biopsy tissue from patients with glioblastoma. We demonstrate that pyrosequencing detection of MGMT methylation has an analytical sensitivity suitable for clinical utility. MGMT methylation assay can provide a useful molecular biomarker for prediction of chemosensitivity in patients with glioblastoma multiforme.

1826 Osteopontin and CD44 Immunoexpression in Primary Central Nervous System Lymphoma, and Comparison with Nodal and Extranodal Diffuse Large B-Cell Lymphoma

J Yuan, K Gu, S Sharma. Medical College of Georgia, Georgia Health Sciences University, Augusta, GA; University Hospital, Augusta, GA.

Background: Primary central nervous system lymphoma (PCNSL) is a diffuse large B-cell lymphoma (DLBCL) mostly of non-germinal center-like (non-GCB) type. Osteopontin, recently the most up-regulated gene in PCNSL, contributes to spread of carcinomas and myeloma by binding to CD44 variants (CD44v), especially CD44v6. We studied immuno-expression of osteopontin, and its putative receptor CD44v6 and CD44H in PCNSL.

Design: We studied 49 archival pathology cases, including 20 PCNSL, 12 N-DLBCL, and 17 EN-DLBCL. Immunohistochemical (IHC) staining was performed for osteopontin (OPN), CD44v6, CD44H, CD10, BCL-6, MUM-1, and Ki67, semi-quantitatively scored by % positivity of tumor cells (0%, 1-25%= score 1, 26-50%=2, 51-75%=3, and 76-100%=4) and staining intensity (none=0, weak=1, moderate=2, intense=3), and an overall IHC score (OIS) obtained by multiplying % score with intensity score (0 to 12), and correlated with Ki67 indices, and GCB vs. non-GCB types.

Results: OPN nuclear positivity was variably observed in 20 of 20 (100%) PCNSL cases, 16 of 17 (95%) EN-DLBCL, and 3 of 12 (25%) N-DLBCL. The OIS of OPN in PCNSL (7.0±3.5) and EN- (4.4±4.1) groups was significantly higher than N-DLBCL (0.3±0.6) ($p < 0.001$). The difference in OPN IHC scores between PCNSL and EN-DLBCL group, was not significant ($p=0.053$). Of the 16 of 49 cases positive for CD44v6 (33%), 6 were PCNSL, and 5 each EN- and N-DLBCL; no statistical difference was observed. CD44H was positive in all cases except one PCNSL, but without any significant differences across the three groups. When non-GCB was compared with GCB group, only CD44H expression was significantly different, with higher expression in non-GCB (score 12±1.5) than GCB group (9.5±3.1) ($P=0.015$); the differences were insignificant for OPN and CD44v6. Neither CD44H nor CD44v6 scores correlated with the OPN expression score or Ki67 index.

Conclusions: Osteopontin immunoexpression was highest in PCNSL (PCNSL > EN-DLBCL > N-DLBCL), suggesting its probable role in its pathogenesis. However, its lack of correlation with CD44v6 excludes any major role of the latter in OPN overexpression in PCNSL. Moreover, no association was observed between proliferative index and expression of OPN, CD44H or CD44v6. The significantly higher CD44H expression in non-GCB than GCB group may contribute to the aggressiveness of the non-GCB DLBCL. Further studies with additional CD44 variants may clarify the prognostic/predictive role of osteopontin in PCNSL.

1827 IMP3 Expression in Astrocytic and Oligodendroglial Tumors

L Zhao, TW Smith, D Lu, H Yu, L Qin, KY Xiao, K Dresser, T Stockl, BA Woda, Z Jiang, S Hao. University of Massachusetts Medical School, Worcester, MA.

Background: Insulin-like growth factor-II mRNA-binding protein 3 (IMP3), an oncofetal protein, is involved in embryogenesis and is expressed in multiple malignant neoplasms. IMP3 has been shown to have higher expression in high grade tumors and is associated with poor prognosis. With the exception of glioblastoma, IMP3 expression in primary brain tumors of glial origin has not been systematically investigated. In this study, IMP3 expression in a series of astrocytic and oligodendroglial tumors is examined and correlated with histologic type and WHO grade.

Design: Two hundred forty-four (244) cases of neurosurgical biopsy and brain resection specimens from 1998-2008 were retrieved from the pathology archives of our institution. The tumors included: 149 cases of glioblastoma (GBM), (WHO Grade IV); 19 anaplastic astrocytoma (Grade III); 35 anaplastic oligodendrogliomas and anaplastic mixed gliomas (Grade III); 14 oligodendrogliomas and low grade mixed gliomas (Grade II); and 17 pilocytic astrocytomas (Grade I). Ten cases of gliosis were used as controls. All cases were stained with a monoclonal antibody specific for the IMP3 protein, and evaluated independently by 3 observers. IMP3 expression was divided into 2 categories: positive (moderate or strong cytoplasmic staining with membranous accentuation, >5%) and negative (absent or weak cytoplasmic staining, <5%).

Results: IMP3 was expressed in 93% (138/149) of GBMs, 79% (15/19) of anaplastic astrocytomas, 26% (9/35) of anaplastic oligodendrogliomas and anaplastic mixed gliomas, and 18% (3/17) of pilocytic astrocytomas. Grade II oligodendroglioma and low grade mixed gliomas (0/14), and gliosis (0/10) showed no IMP3 expression. This expression was statistically significant ($p < 0.05$) between the high grade tumors and gliosis, among the high grade tumors (Grade III and IV), and additionally between each of the high grade tumors and low grade tumors. Among the low-grade (Grade I and II) tumors and gliosis cases, no statistically significant difference in IMP3 staining was found.

Conclusions: IMP3 expression is positively correlated with WHO grade. IMP3 expression is found in the majority of GBMs (Grade IV). Grade III gliomas have a higher percentage of expression than Grade I and II gliomas. IMP3 is expressed more frequently in astrocytic tumors compared to oligodendroglial tumors of the same grade or even higher grade. IMP3 staining is helpful in distinguishing high grade gliomas from low grade ones and gliosis.

Ophthalmic

1828 Twist, E-Cadherin, and Uveal Melanoma Metastasis

WR Bell, A Spitze, L Asnagli, ML Coonfield, CG Eberhart. Johns Hopkins University School of Medicine, Baltimore, MD.

Background: Metastatic spread is the main cause of death in patients suffering from uveal melanomas, but the molecular basis of tumor dissemination is only partially understood. Increased expression of proteins linked to epithelial mesenchymal transition (EMT) have been previously associated with invasion and metastasis in a number of cancers, but they have not been analyzed in uveal melanoma. We therefore examined expression of the EMT-associated protein Twist in uveal melanoma cell lines and in primary tumors. We also analyzed E-cadherin, which is frequently downregulated by Twist in metastatic carcinomas.

Design: Twist expression was analyzed using Western blots of protein extracts from four uveal melanoma cell lines (OCM1, OMM1, OM431), and by immunohistochemical analysis of a tissue microarray containing representative cores from 80 uveal melanomas. At least three intact cores were required for a tumor to be scored. We also examined E-cadherin levels using immunohistochemistry on the tissue microarray. A semiquantitative (0, 1+, 2+, 3+) scale was utilized for the immunohistochemical evaluations.

Results: Twist and E-cadherin were detected in protein extracts from all three uveal melanoma cell lines examined, while E-cadherin was present only in OCM3. Interestingly, the OCM3 cells expressing E-cadherin appeared to spread more slowly than the other two lines examined. Silencing of Twist expression with shRNA resulted in significant reduced invasion *in vitro*. On the tissue array, 72 cases had sufficient evaluable cores for analysis, and 27 of these (38%) had high levels (3+) of Twist. In the same 72 tumors, 18 (25%) had very low or absent (0 to 1+) expression of E-cadherin. Interestingly, 11 of the 18 tumors (61%) with low or absent E-cadherin had high levels of Twist, suggesting that Twist might repress E-cadherin expression in uveal melanoma. Statistical analysis of the immunohistochemical staining data in all 72 cases showed a trend towards a negative correlation between Twist and E-cadherin ($p = 0.06$, two-tailed Spearman test). Twist and E-cadherin expression did not appear to correlate with histopathological factors, metastasis, or overall survival, although clinical follow-up was only available for 25 patients with tumors represented on the array.

Conclusions: High levels of Twist protein expression are more common in uveal melanoma with low E-cadherin, suggesting a potential relationship between the two. However, OCM3 cells co-express both proteins, and the overall negative correlation on our tissue microarray was not statistically significant ($p = 0.06$).

1829 Expression of Sonic Hedgehog Signaling Pathway Related Proteins in Retinoblastoma

J-Y Choe, JY Yun, YK Jeon, SH Kim, JE Kim. Seoul National University Hospital, Seoul, Korea; Seoul National University Boramae Hospital, Seoul, Korea; Yonsei University Hospital, Seoul, Korea.

Background: Sonic hedgehog (SHH) protein is a member of secreted signaling molecules that is involved in early embryonic development of various organs. Dysregulation of this pathway has been reported in several cancers but not yet assessed in retinoblastoma.

Design: Fifty-four cases of retinoblastoma were investigated immunohistochemically using antibodies against SHH pathway proteins such as SHH, GLI1, GLI2, GLI3, and ABC binding cassette G2 (ABCG2) on tissue microarray blocks. Western blot (WB) analysis was performed to confirm the expression of SHH and GLI proteins in two retinoblastoma cell lines, Y-79 and WERI-Rb-1. Correlation between the expression of SHH signaling proteins and various clinicopathologic parameters was statistically analyzed.

Results: SHH was expressed in most cases of retinoblastoma (52 of 54, 96.3%), 10 cases (18.5%) showing strong expression. GLI1 and GLI2 were also highly expressed, 44 of 54 cases (81.5%) and 49 of 53 cases (92.5%), respectively. GLI3, a transcriptional repressor, was expressed in 23 of 54 cases (42.6%) at low levels. ABCG2 expression was found in 12 of 54 cases (22.2%). High expression levels of these proteins in retinoblastoma cell lines were confirmed by WB. Expression of SHH correlated with advanced T stage ($p=0.026$), optic nerve invasion ($p=0.014$), necrosis ($p=0.036$) and distant metastasis ($p=0.029$). Expression of ABCG2, which represents chemoresistance, positively correlated with that of SHH ($p=0.002$).

Conclusions: SHH related proteins are highly expressed in retinoblastoma tumor cells. SHH expression is closely related to advanced disease and overexpression of chemoresistance protein, ABCG2. These findings strongly suggest that SHH signaling pathway may play a significant role in progression of retinoblastoma.

1830 Squamous Cell Lesions of the Conjunctiva: Evaluation of Current Grading Systems and Patho-Epidemiological Survey of Patients in Blantyre, Malawi

KL Golden, DA Milner. Brigham and Women's Hospital, Boston, MA.

Background: Conjunctival squamous cell lesions are an uncommon disease with a variable geographic incidence, being more common in countries closer to the equator.